NOAA OAR Special Report

PMEL Tsunami Forecast Series: Vol. NNNN
Development of a Tsunami Forecast Model for Portland, Maine

Michael C. Spillane [1,2]

[1]Joint Institute for the Study of the Atmosphere and Ocean (JISAO), University of Washington, Seattle, WA
[2]NOAA/Pacific Marine Environmental Laboratory (PMEL), Seattle, WA

September 2009

NOTICE from NOAA

Mention of a commercial company or product does not constitute an endorsement by NOAA/OAR. Use of information from this publication concerning proprietary products or the tests of such products for publicity or advertising purposes is not authorized. Any opinions, findings, and conclusions or recommendations expressed in this material are those of the authors and do not necessarily reflect the views of the National Oceanic and Atmospheric Administration.

Contribution No. XXXX from NOAA/Pacific Marine Environmental Laboratory

Also available from the National Technical Information Service (NTIS)
(http://www.ntis.gov)

Contents

List of Figures

List of Tables

PMEL Tsunami Forecast Series: Vol. NNNN
Development of a Tsunami Forecast Model for Portland, Maine

Michael C. Spillane [1,2]

Abstract. Operational tsunami forecasting by NOAA's Tsunami Warning Centers relies on the detection of tsunami wave trains in the open ocean, the inversion of these data (telemetered via satellite) to quantify their source characteristics, and real-time modeling of the impact on threatened coastal communities. The latter phase of the process involves, for each such community, a pre-tested forecast model capable of predicting the impact, in terms of inundation and dangerous inshore currents, with sufficient resolution and within the time constraints of an emergency situation.

In order to achieve this goal, considerable advance effort is required to tune each forecast model to the specific bathymetry and topography, both natural and manmade, of the impact area, and to validate its performance with a complete set of potential tsunami sources. Where possible the validation runs should replicate observed responses to historical events, but the sparse instrumental record of these rare but occasionally devastating occurrences dictates that comprehensive testing should include a suite of scenarios that represent potential future events.

During the forecast model design phase, and in research mode outside the pressures of an emergency situation, more detailed and slower-running models can be investigated. Such a model (referred to as a Reference Model) represents the most credible numerical representation of tsunami response for the study region, using the most accurate bathymetry available and without the run-time constraint of operational use. Once a reference model has been developed, the process of forecast model design is to determine where efficiencies can be gained, through reducing the grid resolution and increasing the model time step, while still adequately representing the salient features of the more detailed (but not operationally feasible) solution.

This report documents the reference and forecast model development for Portland, which is the major metropolitan area in the state of Maine. At the time of writing, Portland has not experienced a tsunami. This is the result both of the sparse history of events along the eastern U.S. seaboard, and the presence of a broad shallow shelf that isolates the Gulf of Maine from the open Atlantic; Portland itself lies in a sheltered embayment of the Gulf called Casco Bay. The absence of a historical record eliminates the option of model validation based on observations, but the investigation of realistic event scenarios, involving seismic activity north of Puerto Rico or, more remotely, in the south and east Atlantic, suggests that the study area is not immune to impact.

[1] Joint Institute for the Study of the Atmosphere and Ocean (JISAO), University of Washington, Seattle, WA
[2]NOAA/Pacific Marine Environmental Laboratory (PMEL), Seattle, WA

1. Background and Objectives

1.1. The Setting

Portland is a harbor city at the southwest corner of Casco Bay, an inlet of the Gulf of Maine. The city lies on a neck of land between Back Cove to the north and the Fore River estuary to the south. The latter provides a sheltered anchorage with a deep channel, just three and a half miles from the Gulf but sheltered from it by numerous islands as seen in the aerial view of Figure 1. Portland's natural setting has fostered a long history of permanent settlement extending back to 1633 (Conforti, 2005). It's principle exposure is to gales from the northeast and the area has been impacted by numerous storm surge events as well as several hurricanes and tropical storms over the years, as recorded by Cotterly (1996) and Budd (1980).

The city with its neighboring communities, including South Portland on the southern bank of the Fore River (and Biddeford further south), is the largest metropolitan area within a state whose coastline is extremely rugged, with numerous islands and inlets. Its physical beauty makes Maine a desirable vacation destination (with an estimated 3.6 million visitors per year) for which Portland is a hub, thereby adding a sizeable non-resident population. The estimated metropolitan population for July 2008 was 514,065 (www.census.gov/popest/metro/metro.html). While outlying coastal communities, on the mainland and nearby islands, are also exposed to some tsunami risk, the focus of the forecast model is on the main population and infrastructure centers of Portland and South Portland. Figure 2 serves to identify features and locations within the study area that arise in subsequent discussion.

1.2. Natural Hazards

As noted earlier, tsunami impact is low on the spectrum of natural hazards to Maine, as indeed it is for the entire eastern seaboard of the United States. Low, that is, in terms of frequency of occurrence. The area is not immune however; potential sources have been compiled and discussed (AMTHAG, 2008; ten Brink et al., 2009). Historically however, the compilation of tsunami data by Lander and Lockridge (1989) has scant mention of Maine. The largest, most widespread, recorded tsunami in the Atlantic to date was associated with the Lisbon earthquake of 1755. Despite the numerous population centers in colonial America, observations of the event in the western Atlantic were mainly from the Caribbean, with one from Bonavista, Newfoundland (see Figure 3). Barkan et al. (2009) have attributed this to the orientation of the source; other source geometries in future events might pose a greater threat to the U.S. mainland. The largest local earthquake for the east coast, estimated at magnitude 6.3, occurred in the same year (1755) and was centered east of Cape Ann, Massachusetts. Lander and Lockridge (1989) however report only confused accounts of wave activity.

Another significant source mechanism for damaging tsunami waves is submarine landslide (Driscoll et al., 2000). Portland, and a number of other Maine locations are listed as having experienced "high tides" following the submarine landslide-induced

tsunami of 1929 whose source was south of Newfoundland and led to serious loss of life and damage there. A study of the event by Fine et al. (2005) and an extensive search by Wigen (1989) revealed no instrumental records of water level response from Maine, though the tsunami signal was evident in the Atlantic City, NJ tide gage. Figure 3, in addition to locating Portland in its North Atlantic context, identifies potential tsunami sources. The locations of the BPR instruments of the U.S. DART® array, capable of detecting propagating tsunami waves in the open ocean, are marked. By transmitting direct observations via satellite, DART®s initiate the process culminating in real time forecasts. Two nearby communities for which forecast models will be developed (Portsmouth, NH and Bar Harbor, ME) are marked in the upper left inset.

The Lander and Lockridge (1989) tsunami catalog includes a number of unexplained events. In 1872 Penobscot Bay experienced waves of up to 50cm for which a seismic source has not been identified. On January 9, 1926 Bass Harbor on Mt. Desert Island, ME emptied suddenly then a 3-meter inrush of water followed; a lesser wave was observed the same day at Vinalhaven in Penobscot Bay. On October 28, 2008 anomalous harbor oscillations, reminiscent of Bass Harbor 1926, were experienced at Boothbay, Southport, and Bristol, ME, as reported in the Boston Globe (2008). Speculation about the origin of the latter occurrence includes the possibility that it might be meteorological. Several tide gages between New Jersey and Maine show weaker but consistent oscillations associated with the passage of an offshore weather system. A squall-line surge was posited (Sallenger et al., 1995) as the source of an unusual wave in Daytona, FL in July 1992. Other areas of the world are prone to meteorologically-forced tsunamis, referred to locally as “šćiga” in the Adriatic or “rissaga” in the Balearic Islands The theory of such waves is described by Monserrat et al., (2006) where some dramatic images of their effects are shown.

1.3. Tsunami Warning and Risk Assessment

The forecast model development, described here, will permit Portland, ME, to be incorporated into the tsunami forecasting system SIFT, developed at NCTR (NOAA Center for Tsunami Research) for use by the U.S. Tsunami Warning Centers (TWC’s). Currently that system is focused on seismically-generated tsunamis but the existence of a tested model for Portland, ME should allow non-seismic sources, landslide or meteorological, to be added as methodologies to simulate them become available.

As noted earlier, a more frequently recurrent natural hazard for Portland, and other communities in the Gulf of Maine, is storm surge. Forecast and warning tools are available, based on the Gulf of Maine Ocean Observing System (www.gomoos.org), to inform emergency managers when the threat of such an event is perceived. The amplitudes (~ 1m) of the largest tsunami waves, simulated in this report, may not sound overly serious, compared with the surges that are not uncommon for the area. However the sudden onset and rapidly varying and damaging currents of a tsunami make their inclusion in a comprehensive warning capability important in an area of extensive waterfront infrastructure. In this regard the forecast model, and its associated tools, will be of benefit in ongoing risk assessment; adjustments to the bathymetric files can be

made to mimic proposed developments, such as dredging or near shore construction, to investigate how they might alter the harbor response.

2. Forecast Methodology

2.1 The Tsunami Model

In operational use, a tsunami forecast model is used to extend a pre-computed deep-water solution into the shallows, and onshore as inundation if appropriate. The model consists of a set of three nested grids, of increasingly fine resolution, that in a real-time application of the MOST model [Method of Splitting Tsunami: Titov and Synolakis, 1998; Titov and Gonzalez, 1997) permits forecasts at spatial scales (as little a few tens of meters) of relevance to local emergency management. The validity of the MOST model applied in this manner, and the operational effectiveness of the forecast system built around it, has been demonstrated during unplanned tests triggered by several mild to moderate tsunami events in the years since the 2004 Indian Ocean disaster (Wei, 2008). Successful hind casting of historic tsunamis, during the forecast model development for communities in the Pacific basin with an instrumental record of their impact, lends credence to forecasting of major events. Such validation of tsunami modeling procedures is documented in other volumes of the series of which this report is but one. Before proceeding to a description of the forecast model development for Portland, it may be useful to describe the steps in the overall forecast process.

2.2 The SIFT Forecast System

Operational tsunami forecasts are generated at Tsunami Warning Centers, staffed 24/7 in Alaska and Hawaii, using the SIFT (Short-term Inundation Forecasting for Tsunamis) tool, developed at NCTR. The semi-automated process facilitates the steps by which TWC operators assimilate data from an appropriate subset of the DART® tsunami sensors, "invert" the data to determine the linear combination of pre-computed propagation solutions that best match the observations, then initiate a set of forecast model runs if coastal communities are threatened or, if warranted, cancel the warning.

Steps in the process are as follows:

- When a submarine earthquake occurs the global network of seismometers registers it. Based on the epicenter, the unit sources in the Propagation Database (Gica et al., 2008) that are most likely to be involved in the event, and the DART® array elements (Spillane et al., 2008) best placed to detect the waves passage are identified. TWC watch-standers can trigger DART®s into rapid sampling mode in the event that this did not occur automatically in response to the seismic signal.
- There is now an unavoidable delay while the tsunami waves are in transit to the DART®s; at least a quarter of a cycle of the first wave in the train must be sampled before moving to the "inversion" step.
- When sufficient data have accumulated, at one or more DART®s, the observed time series are compared with the model series from the candidate unit sources. Since the latter are pre-computed (using the MOST code), and the dynamics of tsunami waves in deep water is linear, a least squares approach taking very little time can identify the unit sources, (and the appropriate scale factors for each,) that

best fit the observations. The "inversion" methodology is described by Percival et. al., (2009).

- Drawing again on the Propagation Database, a composite basin-wide solution is available with which to identify the coastal regions most threatened by the radiating waves.
- It is at this point that one or more forecast models are run. The composite propagation solution is employed as the boundary condition to the outermost (A-grid) domain of a nested set of three real-time MOST models that telescope with increasingly fine scale to the community of concern. A-grid results provide boundary conditions to the B-grid, which in turn forces the innermost C-grid. Non-linear processes including inundation are modeled so that, relying on the validation procedures during model development, credible forecasts of the current event are available.
- Each forecast model provides quantitative and graphic forecast products with which to inform the emergency response, or to serve as the basis for canceling or reducing the warnings. Unless the tsunami source is local, the forecast is generally available before the waves arrive but, even when little or no lead-time can be provided, the several hour duration of a significant event (in which the first wave may not be the most damaging) give value to the multi-hour forecasts provided.

Because multiple communities may be potentially at risk, it may be necessary to run simultaneously, or in a prioritized manner, multiple forecast models. Each must be optimized to run efficiently in as little time as possible; the current standard is that an operational forecast model should be capable of simulating 4 hours of real time within about 10 minutes of CPU time on a fast workstation computer. Due to the presence of a broad and shallow shelf between Portland and the deep ocean south of Georges Bank, which slows the waves, this standard is difficult to attain. The slow passage across the shelf requires that 8-12 hours be simulated from the time when the wave train enters the A-grid domain. On the other hand by delaying the arrival and reducing the waves amplitude, the broad shelf reduces the urgency of producing a forecast. Should estimates and observations from more exposed sections of coast be mild, a decision to terminate the Portland model run may be justified.

3. Forecast Model Design for Portland, Maine

3.1 Digital Elevation Models

Water depth determines local tsunami wave speed and sub-aerial topography determines the extent to which tsunami waves inundate the land. Thus a prerequisite for credible tsunami modeling is the availability of accurate gridded bathymetric and topographic datasets, termed DEMs (Digital Elevation Models.) Given their expertise in this area, and the number of coastal communities needing tsunami forecast capability, NCTR relies heavily on the National Geophysical Data Center (NGDC) to provide the DEMs required. In the case of Portland Maine, the DEM, a composite of multiple data sources merged and converted to a common datum of Mean High Water (MHW), was produced and documented by Lim et al. (2008). The use of MHW as the "zero level" for forecast results is standard. The MOST model does not include tidal fluctuations and, since a tsunami may arrive at any stage of the tide, it is best to employ a "worst-case" approach by assuming high tide when forecasting impacts.

The DEM provided by NGDC for Portland is illustrated in Figure 4. For a thorough description of the data sources and methods employed in constructing it, see Lim et al. (2008) whose Table 1 is reproduced below. With one-third arc second (~10m) resolution the DEM provides the basis for the B and C-grids for both reference and forecast model usage. NCTR maintains an atlas of lower resolution gridded bathymetries, which can be used for the A-grids, as described later.

3.2 Tides and Sea Level Variation

Portland has a history of tidal observations dating back to 1910. The tide station (8418150) is located at the south end of State Pier and the instrumentation has been upgraded to include a tsunami-capable gage sampling at one-minute intervals. Station characteristics are provided in Table 2, based on the wealth of online tidal information available at NOAA's CO-OPS (Center for Operational Oceanographic Products and Services) website (tidesandcurrents.noaa.gov). Note the sizeable diurnal range of over three meters and that, while the rate of change in sea level is low (compared to more seismically active areas), there is substantial seasonal, interannual and short-term variability.

A sample section of the tide gage record, again extracted from the CO-OPS website is reproduced in Figure 5. Deviations (or residuals) from the astronomically predicted tide can be several tens of centimeters. A recent NOAA Technical Report (Sweet et al., 2009) has studied the widely reported anomalous sea level elevations along the U.S. East Coast during June-July 2009. They attribute the anomalies (which when smoothed were as much as 10mm above seasonally adjusted levels in the case of Portland) to northeasterly wind forcing and changes in Gulf Stream transport. The final rows of Table 2 refer to the threshold for coastal flooding employed in producing storm surge warnings for the coast of Maine. Since MHW is 2.886m above MLLW and the threshold (of 3.658m) used in

storm surge modeling has been exceeded about 37 times since 1980 (Cannon, 2007), the use of MHW as the zero level of modeled sea level may not be the truly worse case. While the simultaneous arrival of the crest of a large tsunami at high tide during a storm surge has low probability, a feature of the simulated events reported below is that sustained harbor oscillations at a resonant period (a mild instance of which is shown in Figure 5) may extend the duration of the threat. This frequently occurs at Crescent City, CA (as discussed later using Figure 12.)

To look for resonances in sea level in the Portland area, a five lunar month record (Jul. 29, 2008 to Feb. 1, 2009) of one-minute data was down-loaded from the CO-OPS website. Several short gaps in the record were patched by interpolation of the six-minute instruments and the predicted tidal signal was subtracted. A spectral analysis using the FFT (Fast Fourier Transform) of the residuals produced the spectrum shown in red in Figure 6. Several peaks, at frequencies associated with tidal constituents are evident (particularly M2) when the results are band-averaged, indicating that a low level of tidal energy has not been eliminated by the predictions. Beyond the shallow water tidal constituents is where our interest lies. Here a clear peak with a period about 94-minutes and several lesser peaks appear; one of these, near 12-minutes is apparent in the sample record shown in Figure 5. Oscillations at this and other periods were observed visually during the downloading of the tidal data but appeared quite episodic and the noisiness of the spectrum is not surprising. From the synthetic time series at the tide gage site, generated from numerous forecast model runs (see Section 4), an ensemble average spectrum drawn in blue in Figure 6 was constructed and the correspondence between several of its peaks with those in the observed spectrum will be discussed later.

3.3 The CFL Condition and other grid design considerations

Water depth-dependent wave speed, in conjunction with the spacing of the spatial grid representation, place an upper limit on the time step permissible for stable numerical solutions employing an explicit scheme. This is the CFL limit (Courant-Friedrichs-Levy), which requires careful consideration when the grids employed for a reference or forecast model are being designed. Finer-scale spatial grids or greater water depths require shorter time steps, thereby increasing the amount of computation required to simulate a specific real time interval.

Another feature of the application of gridded numerical solutions to the tsunami wave problem is the shortening that the wave train encounters in moving from deep water onto the shelf. In deep water a grid spacing of 4 arc-seconds (of latitude and longitude, corresponding to ~7km) is typically used to represent propagating wave trains whose wavelength is typically of the order of a few hundred kilometers. The stored results of such propagation model runs are typically decimated by a factor of 4, resulting in a database of ~ 30km spacing (and 1 minute temporal sampling) with which to generate the boundary conditions for the outermost of the nested grids in a model solution. The extraction of the boundary conditions (of wave height and the two horizontal velocity components) is achieved by linear interpolation in space and time. To provide realistic interpolated values the stored fields for these variables must be smoothly varying, and

have adequate sampling in space and time to resolve their structure. As seen in Figure 7, the steep rise of the seafloor along a north south transect (68^0W) from the abyss to Georges Bank is likely to preclude the use of coarsely resolved grids. After some experimentation, placing the southern boundary of the A-grid at 37^0N was found to permit adequate interpolation.

Figure 8 is used to illustrate the shortening and slowing that a wave train encounters as it moves onto the continental shelf, Ideally an animation of model waves would be provided but this is not possible in a printed report. Instead travel time contours (isochrons), based on the TTT (Tsunami Travel Time) application (Wessel 2008), are drawn at 10-minutes intervals for waves originating near Puerto Rico. The isochrons, which mimic wave fronts, become compressed drastically as they "move" onto the shelf. Another benefit of this presentation is that it illustrates the extended duration of the simulation time required; waves traversing the broad shallow shelf take approximately 4 hours (after first encountering the model domain boundary) to reach the interior of Portland harbor, shown in the inset (where the contour interval has been reduced to 1-minute.). As the forecast model results will illustrate, the tsunami wave train, and the harbor oscillations it excites, persist for several hours so that at least 8 to 12 hours of simulation are required.

The isochrons in the inset panel of Figure 8 show the possibility of waves entering the C-grid by the shallower northern entrance. However the TTT calculation is strictly geometric, based on water depth alone, and does not indicate the importance of this mode of entry. A hydrodynamic model, such as MOST, is needed to elucidate the energetics.

In consequence of the above discussion, the outer boundary through which the waves enter the study region should be placed in the deep water off the shelf in order to allow the propagation database-derived boundary values to transition smoothly into the model interior. The outermost A-grid of the nested needs to have fine enough resolution to adequately represent the compressed waves as they move onto the shelf to become the boundary condition forcing the intermediate B-grid. Another feature illustrated by Figure 8 is the wave refraction associated with depth changes. Waves move more rapidly into the Gulf of Maine through the deeper channel to the east of Georges Bank. A shallower region to the west also eases entry and the waves tend to converge in the lee of the bank. Some tsunami energy is reflected by the steep continental rise (Figure 7) but the portion that enters the Gulf is essentially trapped and can set up sustained oscillations, that impact the embayments that lead from the Gulf, until finally dissipated by friction.

As yet the placement of the eastern boundary of the A-grid has not been discussed. As implied by the color contouring of Figure 8, most of the eastern boundary lies in deep water. Though of less concern for waves of Caribbean origin, which arrive from the south, those from the east and southeast can in part enter along the shelf. The fastest waves will however be those traversing deep water so the earliest waves that enter the C-grid should be the most accurately represented. Later waves, some of whose paths have taken them along the shelf, where coarser A-grid bathymetry may not as accurately reflect the physics, may be less well modeled. In the case of Portland there are no

observations for validation but, in comparisons of reference and (coarser) forecast model solutions, it should not come as a surprise if they agree better in the early portion of a simulation.

Another set of considerations comes into play in choosing the placement of the B-grid boundary. Portland, in addition to benefiting from the broad shallow shelf of the Gulf of Maine, is further sheltered by the many islands studding Casco Bay. An adequate resolution to represent such islands and entrances leading to the city will, as far as possible be confined to the innermost C-grid. The outer boundary of the B-Grid will be placed well outside this so that it can provide a reasonable transition from the A-grid domain to the approaches to the C-grid. A B-grid encompassing the entirety of Casco Bay has been selected, extending from near Cape Elizabeth in the south to Cape Small in the northeast.

3.4 Specifics of the model grids

After several rounds of experimentation, the extents and resolutions of the nested grids chosen are as illustrated in Figures 9 and 10, and Tables 3 and 4. The reference and forecast grid pairs (at the A and B levels) have the same extent, differing only in resolution; the C-grid domain is slightly larger for the reference model than for the forecast model, the upper reaches of the Fore River and the Presumpscot Estuary being eliminated in the latter. The parent grids were sub-sampled at their nodes, rather than interpolated, with some smoothing and editing where necessary to eliminate erroneous points or grid features that tend to cause model instability. For example, "point" islands where an isolated grid cell stands above water are eliminated, as are narrow channels or inlets one grid unit wide; these tend to resonate in the numerical solution. Large depth changes between adjacent grid cells can also cause numerical problems; customized tools (such as "bathcorr") are available to correct many of these grid defects. In other situations some "sculpting", particularly of the lower resolution grids, was necessary to retain important features such as causeways, jetties and deep-water channels that may have been poorly represented or eliminated by the sub-sampling.

A naming convention "region_resolution_purpose.type" was adopted for the gridded files. Here "region" is "GulfME", "CascoBay", or "PortlandME" for the A, B, or C grids respectively. Where possible, easily understood abbreviations such as "1m", "30s" are used to identify the resolution; where fractional arc-second steps occur "$^1/_3$ arc-second" and "$^4/_3$ arc-second" are denoted by "1th" and "4th"respectively. In the interests of reducing the run-time requirement of the forecast model, differing angular resolutions in the zonal and meridional directions are employed. At the latitude of Maine, a 4:3 ratio of longitude:latitude grid increments produces grid cells that are nearly square in distance units (1.367 rather than 4:3 is the ideal.) The abbreviation "120s90s" represents a grid with 2 arc-minute zonal increments, but 1.5 arc-minute meridional steps. The "purpose" portion of the name is either "r" (reference) or "f" (Forecast) as appropriate. The file "type" designator is either ".most" or ".nc". The former refers to the ASCII raster format employed in the current version of MOST in which the header records (defining the number of columns and rows and the axis coordinates in decimal degrees) are followed

by raster records (with depths positive), ordered from north to south. To facilitate post-processing of model output (as well as the "sculpting" phase of grid creation) netCDF (".nc") formatted bathymetric files, in which water depths are negative and the ordering is south to north, are preferred by the author and are available on request.

Details of the model grids are provided in Tables 3 and 4. The latter lists the maximum depth, the CFL time step requirement that must not be exceeded, and the actual time steps chosen for the reference and forecast model runs. Since in the current version of MOST, employed by SIFT, the numerical solutions in the three grids proceed simultaneously, there is a requirement that the A and B-grid time steps be integer multiples of the (innermost) C-grid time step in addition to satisfying the appropriate CFL requirement. For both reference and forecast models the CFL requirement of the C-grid was the most stringent. The values chosen are shown in the fifth column of Table 4 and are such that an integer multiple of each time step (16x for the forecast model; 64x for the reference) is identically 30 seconds, the chosen output time interval for both models.

The reference model grid files are illustrated in Figure 9; those for the forecast model in Figure 10. In printed form it is difficult to distinguish between them, other than that the "forecast" version of Grid-C the domain is slightly smaller. This was done largely to eliminate the influence of Long Creek, just upriver from the I-295 bridge (see Figure 2). The portion of the creek where it enters the Fore River is extremely narrow and, in its low-resolution digitized version behaves in a manner that appears non-physical. On a rising wave, water enters the wider upstream portion of the creek but as the wave ebbs that (model) water cannot escape and the level rises with each cycle. Though not effecting the overall dynamics of the model, the unrealistic level of Long Creek can influence the reported minimum/maximum levels of the model output. As indicated in Figures 2 and 9, the Fore River channel narrows considerably beyond Long Creek and, while the behavior of this stretch appears reasonable in the reference model, excluding it from the forecast version loses nothing of importance. For the same reason the upper reaches of the Presumpscot River Estuary are eliminated in the forecast model.

With the 12-fold reduction in the number of water grid cells, and a 4-fold increase in time step, there is an expectation that a reference model run should take about 48 times longer than the forecast model (10.8 minutes per 4 hours of simulation); this is borne out by experience. It is possible that further reductions in the extent and/or resolution of the C-grid could produce results that are not obviously worse than those reported here. Earlier C-grids that terminated at Mackworth Island were first explored, so as to focus on the more densely populated areas; this was before the dramatic response of the inlet north of the causeway was discovered. Those runs, and others with reduced resolution, could halve the forecast model run time requirement but the extent to which the quality or utility of the product was degraded was not fully tested.

3.5 Model Run Input and Output Files

In addition to providing the bathymetry file names and the appropriate time step and A, B grid, the user must provide a number of additional parameters in an input file. These include the Manning Friction Coefficient, a depth threshold to determine when a grid point becomes inundated, and the threshold amplitude at the A-grid boundary that will start the model. An upper limit for wave amplitude within the model is specified in order to terminate the run if the wave amplitude grows beyond reasonable expectation. Standard values are used: 0.0009 for the friction coefficient and 0.1m for the inundation threshold. The latter causes the inundation calculation to be avoided for insignificant water encroachments that are probably below the uncertainty in the topographic data. Inundation can, optionally, be ignored in the A and B-grids, as is the norm in the (non-nested) MOST model runs that generate the propagation database. When A and/or B-grid inundation is excluded, water depths less than a specified "minimum offshore depth" are treated as land; in effect a "wall" is placed at the corresponding isobath. When invoked, a value of 5m is applied as the threshold, though A and B inundation is normally permitted as a way to gain some knowledge of tsunami impact beyond the scope of the C-grid domain. Other parameter settings allow decimation of the output in space and/or time. As noted earlier, 30-second output has been the target and output at every spatial node is preferred. These choices avoid aliasing in the output fields that may be suggestive of instability, (particularly in graphical output) when none in fact exists.

Finally the input file (supplied in the Appendix) provides options that control the output produced. Output of the three variables: wave amplitude, and the zonal (positive to the east) and meridional (positive to the north) can be written (in netCDF format) for any combination of the A, B, and C-grids. These files can be very large! A separate file, referred to as a "SIFT" file, contains the time series of wave amplitude at each time step at discrete cells of a selected grid. Normally the time series at a "reference" or "warning point", typically the location of a tide gage, is selected to permit validation in the case of future or historical events. Also output in the SIFT file is the distribution of the overall maximum wave amplitude and speed in each grid. By contrast with the complete space-time results of a run, the SIFT file (also netCDF) is very compact and, if more than a single grid point is specified, a broader view of the response is provided. The input files used in model development employ 30 output locations; 25 of these are at points of interest within the C-grid.

By default two additional output files are generated: a listing file, which summarizes run specifications, progress, and performance in terms of run time. Also included in this file is information to determine the reason should a run not start, or terminate early. Finally a "restart" file is produced so that a run can be resumed, beginning at the time it ended, either normally or by operator intervention.

The input files described above are specific to the model itself. For an actual run, the program must be pointed toward the files that contain the boundary conditions of wave amplitude (HA), and velocity components (UA, VA), to be imposed at the A-grid boundary. Time varying conditions are generally extracted as a subset of a basin-wide propagation solution (either a single unit source or several, individually scaled and linearly combined) that mimic a particular event. Alternately a customized source, such

as one of those constructed as scenarios for the Lisbon 1755 event, can be employed. These boundary-forcing files typically consist of 24 hours of values (beginning at the time of the earthquake), sampled at 1-minute intervals and available on a 16 arc-minute grid. Occasionally, for more remote seismic sources (or when delayed arrival of secondary waves due to reflections as has been seen at Hawaii,) the time span of the propagation run available for forcing is extended beyond one day.

4. Model Stability Testing

Before proceeding to an extensive suite of model runs, that explore the threat to Portland from various source regions, the stability of the model is tested in both low and extreme amplitude situations. The former we refer to as "null source" testing: where the boundary forcing is at such a low level (but not precisely zero of course) that the response is expected to be negligible. These tests can be highly valuable in revealing localized instabilities that may result from undesirable features in the discretized bathymetric representation. Inlets or channels that are only one grid cell wide may "ring" or resonate in a non-physical way in the numerical solution. An instability may not grow large enough to cause the model to fail but, in a run with typical tsunami amplitudes, may be masked by actual wave variability.

Forcing by extreme events should also be tested. In addition to the need to test model stability under such circumstances, there is a parameter in the input file that truncates the run if a prescribed threshold is exceeded. For operational use, the threshold must be set high enough so that an extreme event run is not unnecessarily terminated. Both null and extreme-case trials should be done for test sources whose waves enter the model domain from different directions since, although stable for one set of incoming waves, an instability may be encountered for another. The "null" and "extreme" testing of the forecast (and reference) model is reported in the following subsections. Further evidence of stability is provided by the extensive set of scenarios, aimed at exploring the dependence of impact to Portland on source location, described later in the report, and in independent testing by other members of the NCTR group before the model was released for operational use. Table 5 summarizes the synthetic tsunami scenarios tested by the author of this report.

4.1 The "Null" Tests

Three null test cases were run representing sources in the Caribbean, South Atlantic, and Eastern Atlantic. Those based on sources from the propagation database (Caribbean and South Sandwich areas) were scaled down by a factor of 10,000 so as to mimic an M_w=4.8333/Slip 0.0001m source rather than the M_w=7.5/Slip 1m standard. For the Eastern Atlantic, where candidate representations of the Lisbon 1755 event have been explored, a similar downscaling was applied to the "Cadiz Wedge" scenario. Under normal circumstances such weak sources ought not generate a significant response. Several instability-prone features were detected: south of Cottage Cove and between the offshore islands, near Fort Gorges, Long Wharf (west of State Pier), the Casco Bay Bridge, and the north end of the Presumpscot Estuary. Judicious editing of the small-scale features in these areas eliminated the problems. In the B-grid a number of the narrow channels in the north and northeast were sources of localized instability. Some editing removed the problem; nonetheless some of the highly responsive areas undoubtedly reflect reality. Harbors with narrow inlets are where instances of unusual wave activity (mentioned in the Section 1) have been reported, and the funnel-shape of Penobscot Bay, to the east of the B-grid domain, has been identified by Maine's Emergency Management Agency (www.maine.gov/mema) as being particularly

vulnerable to storm surges. Since these areas are not the focus of this study, and would require more detailed bathymetry to accurately represent them, the editing to eliminate their potential to cause instabilities is justifiable. A limited number of grid cells in the outermost (A) grid required correction. Generally these were associated with non-physical features in the DEM, such as where a track of ship-based soundings were improperly merged with other data sources. After a tedious iterative process of grid correction and re-testing with the "null" sources, the testing of large events can begin.

4.2 The Extreme Case Tests

As will be demonstrated later, the east-west aligned portion of the Puerto Rico Trench has the greatest potential for generating tsunamis damaging to the U.S. East Coast. Various USGS studies of earthquakes in the region employ M_w=9 as an extreme. To simulate such a tsunami source, nine A-B pairs of unit sources are used with an evenly distributed slip of 9.86m in each. The geometry of the unit sources, and layout of the propagation database, are described by Gica et al. (2008). Each represents a 100x50km area of the fault surface with the long axis parallel to the plate boundary. The B-row is shallowest, sloping from a nominal depth of 5km (unless a depth estimate has been provided by the USGS based on the earthquake catalogs), row-A is deeper, followed by rows Z, Y, X, … where appropriate. Thus the extreme case source represents a 900km long rupture with a width of 100km. Sources with magnitude M_w=9 were also constructed to represent waves generated in the south and east Atlantic. The former is derived from unit sources along the South Sandwich Island subduction zone; the latter is one of the scenarios (the "Cadiz Wedge") employed to represent the 1755 Lisbon in other NCTR research.

The simulated response of water level at the Portland tide gage to these extreme, or "mega-tsunami" events, is illustrated in Figure 11a. Two curves are drawn for each scenario: those from the reference model are drawn in red, those from the forecast model in green. Figure 11b provides some background to the three sources. The Caribbean source (centered on unit source B51) has a beam pattern (the contours are at logarithmic intervals) that directs a significant proportion of its energy northward, though the greatest impact on the U.S. is in the Carolinas toward which the bathymetry offshore of Cape Fear acts as a wave guide. The Gulf of Cadiz source, whose major lobes include one that impinges on Florida, has a lesser one lobe directed at New England. The main lobe of the South Sandwich source does favor New England.

As this is the first set of simulation results presented in this report, and in the absence of any historical tsunami observations for comparison, it is appropriate to examine the nature of the curves in Figure 11a, and to judge if the forecast model is performing adequately. The first feature that stands out is the highly oscillatory nature of the predictions. Less obvious is that at least two periods of oscillation appear to coexist in each of upper two records. The longer period signal matches that of the first wave to arrive, which appears to trigger a set of shorter period oscillations that persist for some time, partially obscuring the longer period signal until it re-emerges later in the record. The longer period signal appears to be in better agreement (between the reference and

forecast solutions) than the shorter period one. The weakest response, of the cases shown, is for the South Atlantic source. Given its remoteness from Portland, this signal is larger than might be anticipated; this is likely due to the mid-ocean ridge "guiding" wave energy into the North Atlantic. Overall, the close agreement between the first wave arrival time and waveform, and overall range of variation of the two model representations (even though the phase is not always well-matched for later waves) suggests that the forecast model is successfully capturing the essentials of the reference model, at least at this single location.

Later we will use spatial Empirical Orthogonal Function (EOF) analysis to decouple these merged signals or "modes", and to establish whether the close agreement, between the model results at the State Pier, holds generally throughout the C-grid domain. For the present, suffice it to say that the model waveforms in Figure 11a are reasonable. Their periods are in approximate agreement with peaks in the spectral analysis of the Portland tide gage record, presented earlier in Figure 6, where it was remarked that a spectrum, derived from model runs exhibits similar peaks. The second piece of evidence is that enclosed harbors, such as that at Crescent City, CA, frequently "ring" in response to even mild tsunamis.

In Figure 12, the de-tided signal at Crescent City following the Kuril Island tsunami of 2006 shows a strong oscillatory response. Partly the result of the Mendocino Escarpment (a sea floor feature offshore that "guides" transoceanic tsunami energy towards northern California,) but also the result of the natural period of the harbor that make background fluctuations commonplace, Crescent City is prone to oscillatory waves and currents that can cause significant infrastructure damage. For these reasons, and considering the care that was taken to exclude local instabilities during the "null event" model tests, we cannot exclude the possibility that the oscillations in Portland's in the "mega-tsunami" simulations (Figure 11a) mimic reality. We now proceed to the EOF analysis, which reinforce this possibility, sheds some light on the partial disagreement between the reference and forecast model solutions, and provides a measure of the extent to which the good agreement at the reference point is true throughout the C-grid. The latter is an important issue, since there are other parts of the harbor that appear to respond more strongly than does the vicinity of State Pier.

4.3 Spatial EOF Analysis

Figure 11a illustrated the predicted time-varying response to extreme events of water level at a single "reference point", the Portland tide gage where, in the event of an actual tsunami, observations would be available to validate the models. Of course the model results contain much more information: the time history of wave amplitude and currents throughout the C-grid, and the coarser B and A grids beyond. Individual time series like those shown in Figure 11a would differ, in amplitude, as perhaps might the degree of agreement, were another location chosen. What is needed is a means to compare the entire reference and forecast model solutions. Spatial Empirical Orthogonal Function (EOF) analysis is natural to this situation since it can identify patterns in the response of the entire harbor.

The technique has widespread application in earth science as well in many other fields, including economics, with alternate names such as Principal Component Analysis (Bond et al., 2003). Basically, given a set of time series, all of the correlations or covariances between them are computed and placed in a matrix. Mathematical techniques transform this matrix to a diagonal form; the linear combinations (eigenvalues) of the series that achieve this encapsulate the commonalities between them. The diagonal elements are termed eigenvalues and their relative sizes reflect the extent to which the "energy" or variance of the entire set of time series is concentrated in the dominant eigenvector modes. It is not necessary to understand the underlying mathematics as computer applications are readily available to perform the analysis and the meaning of the results are easy to appreciate.

In our spatial EOF analysis the time series are the model predictions for each grid cell of the C-grid; the series in Figure 11a represent just one location. Ideally all 280x537 grid nodes (actually only the 54640 water nodes) in the case of the forecast model would be analyzed. The computer memory requirements of this would be excessive and, in any case, our aim is to compare the two solutions. The C-grid output of both model results are sub-sampled every 8^{th} point in longitude and 9^{th} in latitude of the forecast model nodes; this still provides a representative sampling.

In Figure 13 the EOF results are shown for an 18-hour "extreme event" simulation, using the Forecast Model forced by the Caribbean source. Panels A, C, and D show the patterns of the first three modes which represent 56.3%, 20.4%, and 9.9% of the overall variance during the 18 hours of the model run. The color scale in panel A (Mode 1; 56.3%) shows all locations have the same sign. In physical terms this means that all points are rising (or falling) together but with amplitude that is greatest in the north. By contrast in panels C (Mode 2) and D (Mode 3) the color scales have a zero crossing with portions of the domain rising while another is falling. An interpretation might be that Mode 1 represents the peaks and troughs of the tsunami waves, entering the C-grid domain from the southeast, and exciting harbor resonance modes (seiches) represented by Modes 2 and 3 (and other modes perhaps that are less energetic.) Mode 2 is essentially an east-west oscillation, with the area near Portland Head Light rising and falling at opposite phase to the area near Portland itself. Mode 3 is more north south, with the mid-section of the domain of opposite phase to the vicinity of Mackworth Island and the opening to the Gulf of Maine.

Panel (b) of the figure shows the time history of the first three modes; time in hours varies from top to bottom. Mode 1 dominates early on and persists throughout the entire 18 hours of the simulation (the time axis represents time beginning with the synthetic earthquake.) The first wave sets the C-grid domain into higher frequency oscillations, which build then largely decay away, as they interfere and interact with harbor bathymetry. The area beyond – the Gulf of Maine -- is a basin, virtually bounded by Georges Bank and the coastline. This traps energy, incident from the open ocean, which reflects and refracts around inside providing sustained forcing of the side basins such as Casco Bay and the many other inlets the Gulf of Maine contains.

The results of the Reference Model run, decimated to the same subset of grid cells as were used in the analysis described above, were also subjected to EOF analysis. Three dominant modes again emerge, with similar spatial structures, indicating that, over the C-grid as a whole, the Forecast and Reference models are in good agreement. Together with the spectral results described earlier, the EOF results demonstrate a likely physical reality for the oscillations seen in Figure 11a. They are not a numerical artifact of the modeling and their role in accentuating the response both of water level and current speed needs to be taken into account.

Before proceeding to risk assessment we note that in Figure 13 two "hot spots" of high wave amplitude response are evident. The first is Mill Cove, in the Knightville area of South Portland; though not evident in these graphics, the west side of Mill Cove appears to be the most prone to inundation were a severe tsunami to occur. The other location of concern is the north side of the causeway (Andrews Avenue) linking Mackworth Island to the mainland. The causeway, which has only a narrow gap, and the shoreline northward past the Portland Country Club to the Waites Landing area, clearly acts to concentrate harbor oscillations. Other features to note in these images is the extent to which waves propagate up the Fore River, though the Casco Bay Bridge provides a partial barrier, and into other embayments like Back Cove and the Presumpscot Estuary. Other energetic areas (deep blue in panels B and C represents strong response of opposite phase to the dark red) lie near Cottage Cove and the harbor entrance (Mode 2) and the channel between Diamond and Peaks Islands (Jones Wharf.) Later we will see that other areas emerge with enhanced current speed response.

The EOF analysis described above requires that the entire model output be preserved; these are large files and the EOF, even over the decimated subset employed above, requires several minutes of computation (perhaps less in a customized code, rather than the interactive analysis tool Ferret, employed for this report.) An alternate spatial EOF analysis, based on a subset of just 25 grid cells selected near locations of interest, has been tested and provides results consistent with Figure 13. For such a limited set of points, the necessary data can be stored in the "SIFT" output file which preserves the overall maximum fields of wave amplitude and speed in each of the three grids. Typically only the time series at the reference point is stored in the "SIFT" file but perhaps added value to the forecast might be achieved, at negligible cost in computation or storage, by reporting broader measures (perhaps EOF-based) of harbor response than a single point time series.

As a final note on the use of EOF analysis above, the word "empirical" in its name refers to the fact that the "modes" it identifies are derived from the statistics rather than the physics of the situation. As applied above, in the "time domain", the modes are standing waves. While this conforms with the interpretation applied to Modes 2 and 3, it seems less appropriate to Mode 1 where propagation is expected. An EOF analysis in the "frequency domain" to a band of FFT spectral estimates can reveal evidence of phase structure. Some preliminary "frequency domain" analysis of the frequency band corresponding to Mode 1 reveals a signal, with monotonic north to south phase variation

of about one tenth of a cycle (~10 minutes,) accounts for over 97% of the band's energy. Such phase lags are consistent with the TTT contours in Figure 8, and suggest that propagation is sufficiently rapid, compared to wave period, that the use of time domain EOF analysis for Mode 1 is not grossly inappropriate.

5. Risk Assessment

5.1 Further Testing of the Portland Forecast Model

In the report to date, the stability of the forecast model for Portland has been demonstrated based on "null" sources and selected event scenarios. Were observations available, it would be natural to proceed to validate the Portland model with hind casts of historical events. In the absence of such observations, the outstanding success of the SIFT scheme in more tsunami-prone areas, such as the Pacific Ocean basin, both in hind cast mode and real-time application, must serve as a proxy for validation. The SIFT methodology has provided useful and accurate forecasts (in quasi-operational conditions at NCTR during the development phase) for several mild tsunamis in the past five years (Wei et al., 2008), and is presently installed and undergoing testing at the Warning Centers. It also performed well during the damaging tsunami that struck Samoa in September 2009.

Before the Portland Forecast Model is added to SIFT for operational use, it must be exercised with as wide a range of simulated scenarios as possible. Experience by other NCTR forecast model developers has indicated that the MOST model may exhibit instability for some specific combination of event magnitude and location. It would not be good to discover such an issue under emergency conditions. In this section we report on numerous scenarios explored; in addition to checking that no issues are encountered, the tests build up a knowledge base to inform emergency management in the absence of a historical record. This effort is only a "first installment" on a comprehensive risk assessment and validation. In addition to the scenarios run by the author, and reported here, further tests will be made by other members of the group at NCTR, by staff at the Warning Centers, and by others perhaps in training situations. Among the many related tools developed at NCTR is the Community Model Interface for Tsunami, nctr.pmel.noaa.gov/ComMIT/, which provides a highly intuitive graphical environment in which to exercise and explore forecast models for any combination of propagation database unit sources. Were any of these avenues to reveal a problem with the Portland model, its origin (most likely in some quirk of the bathymetric files) would be located and corrected then the revised version re-installed for operational use. The development of the forecast system will be a dynamic process, with new models added (and old ones revisited) from the current list of U.S interests and globally. In the coming years it is expected that further capabilities (for example landslides) will be added as algorithms and methodologies mature.

5.2 Risk Assessment

As mentioned earlier, potential sources of seismically-generated tsunami waves that might impact the U.S. east coast, and Portland in particular, lie in the subduction zones of the Atlantic Ocean: the Caribbean and the South Sandwich Arc, east of Drake Passage. Despite its remoteness, and perhaps the result of the Mid-Atlantic Ridge in guiding tsunami energy into the North Atlantic, South Sandwich areas are as effective in impacting Portland than some of the lesser Caribbean ones.

The situation with regard to candidate East Atlantic sources is not entirely satisfactory. We employ five of the candidate sources for the 1755 Lisbon tsunami. A constraint on such sources however is that they not direct much energy toward North America. While waves were detected in the Caribbean area of the western Atlantic at the time, no observations were reported from colonial population centers of North America (an exception is Bonavista on Newfoundland.) The non-existence of reports of the 1755 tsunami in North America has been discussed, by Barkan et al., (2009) who also investigated the role of the source orientation on potential impacts to the U.S. Such an approach may be needed to make our risk assessment and stability testing more comprehensive. Clearly relying on East Atlantic sources designed to *not significantly impact* North America is a weakness that must be addressed in future testing and risk assessment.

5.3 Potential Impacts to Portland

Figure 14 illustrates the maximum amplitude at the Portland reference site (the Tide Gage at the south end of the State Pier) in response to a set of 45 magnitude 8.83 scenarios. Where unit sources are available, the source is composed of five A,B pairs with uniformly distributed slip; the Portland response is indicated by color-coding the central member of the 500x100km source group. The group centered on B51 generates a 40cm wave at the Portland tide gage, essentially the same as the “extreme” Caribbean source. The latter was also centered at B51 but the slip was distributed across nine source pairs rather than five and the spread in direction diluted the effectiveness of the greater source magnitude. All Caribbean groupings of the outer tier, from Cuba to Trinidad were exercised and a selection of those within the Caribbean. In particular the Muertos Trough source grouping immediately south of Puerto Rico, with egress to the Atlantic via the Mona Passage, and a grouping further west aligned with the Windward Passage are included. Others, near Panama and north of Columbia and Venezuela where included because their orientation suggested a greater potential to be felt outside the basin.

For the South Sandwich source and the five scenarios representing the Eastern Atlantic the Portland impacts are represented in the inset panel of Figure 14. The East Atlantic sources, based as they are on non-standard shapes and variable slips were scaled up to 8.83 magnitude for consistency. It should be noted that, in all of the simulations used to produce Figure 14 and generate the ensemble-averaged model spectrum in Figure 6, the runs were truncated at 8 hours beyond the time at which a significant wave reached the A-grid boundary. In light of the time that elapses before the waves penetrate to the State Pier, and the extended duration the response of the Gulf of Maine may have (see Figures 11 and 13), there is no guarantee that the maximum amplitude has in fact been reached.

The pattern apparent in Figure 14 is that the northern tier of Caribbean sources, particularly those with an east west orientation and unscreened by offshore islands, have the greatest impact on Portland, producing wave amplitudes of up to 40cm at the State Pier tide gage. The impact declines significantly in moving toward the Lesser Antilles where the main lobe (or "beam") of the tsunamis energy distribution is increasingly directed to the northeast and east. Sources within the Caribbean basin, even those with an east-west orientation or access to the Atlantic via the Mona and Windward Passages are significantly degraded in their threat to Portland. Eastern Atlantic sources with M_w = 8.83 (with the caveat that epicenter location and orientation have not been fully sampled) pose a limited threat. The Gulf of Cadiz source (even for the M_w = 9.0 "mega" event illustrated in Figure 11a) produces oscillations of less than 20cm, though a more comprehensive measure of the threat should include statements regarding inundation and maximum speeds. Neither do South Atlantic sources appear of concern, though a South Sandwich source produces waves of several centimeters, larger than might be expected given its remoteness. As indicated in Figure 11b the latter is likely the result of the beam pattern of the tsunami, guided by the Mid-Atlantic Ridge, directing a sizeable energy "lobe" toward New England.

The forecast model was exercised further with each of the 92 B-row unit sources of the Caribbean in turn (simulating magnitude 7.5 events), in groups of three rescaled and linearly combined to mimic magnitude 8.0, and groups of five to represent magnitude 8.5. No stability problems were encountered and the general pattern of relative impact to Portland, portrayed in Figure 14, was replicated both at the State Pier and at other locations within the C-grid.

5.4 Inundation and Extreme Speeds

Finally, to complete this partial risk assessment, the potential for inundation or hazardous current speeds is explored. Figure 15 displays the maximum amplitude and maximum current speed distributions for the "extreme event": magnitude 9.0, centered at the unit source pair A-B 51. For wave amplitude the areas that also came to light in the EOF analysis stand out. Mill Cove, an inlet in the Knightville area of South Portland, stands out and, unlike in the previous graphics its potential for significant inundation is evident. North of Mackworth Island is also an area subject to high wave amplitudes associated with high frequency oscillations. For high speeds, channels and areas near headlands are most at risk. Among the latter are the sites of the Portland Breakwater and Spring Ledge Lights that bracket the oil tanker jetty that is the terminus of the Portland-Montreal Pipe Line. Strong currents or extreme water level excursions would pose a severe threat to this facility. Some of these issues and locales are briefly discussed in the following section, but not at the level that would constitute a thorough risk assessment.

6. Discussion and Conclusions

The Forecast Model (and the associated Reference Model) described in this report will permit Portland to be added to the coastal communities for which forecast capability is available, and as a tool for use in risk assessment and the evaluation of the impact of waterfront development. Although no historical observations exist with which to validate the models, their behavior in test scenarios suggest that they produce realistic and consistent results. The Forecast Model is an optimized version of the Reference Model that, with reduced spatial resolution and time step, can run within the constraints of an emergency situation while reproducing the main features of the latter. Though the Forecast Model run time of just over 10 minutes per four hours of simulation meets the standard, the location of Portland deep within the Gulf of Maine means that several hours of simulation are needed before waves reach the harbor. Conversely of course this delay, and associated damping of the waves, may allow the lack of damaging waves at other locations to eliminate the need for a Portland run to be completed.

Considerable effort was involved in eliminating artifacts in the digitized bathymetry that generate instabilities: single point islands, single grid cell wide channels or inlets, and severe depth changes between adjacent points. Nonetheless users should be aware that some combination of incoming waves may trigger a numerical resonance and require adjustment to the bathymetry files. Such discoveries would hopefully be made during use of the model for risk assessment, research, or training rather than under operational conditions.

Portland to date has not experienced a tsunami, though is not a stranger to storm surge. The model described in this report adds tsunami forecast and assessment capability to the existing storm surge warning available through GoMOOS. Though both natural hazards involve water level changes, they differ in the time scales they involve. Tsunamis have the potential to arrive with little warning and the time scales of the water movements may, as has been the experience at Crescent City, CA, induce extreme current speeds more damaging than the inundation. Given the extent of water-related recreational activity and infrastructure in the Portland area, tsunamis should be included in emergency planning.

A number of specific locations of concern were identified during the development and testing of the Portland models. Mill Cove is indicated as likely to experience greater water level changes than normal. Interestingly Mill Creek Park at its south end was the site of a tide-driven gristmill in colonial times. Built in 1727 (DiPhilippo, 2007) and operational for many decades, this is among the locations where the Lisbon tsunami of 1755, had it impinged on New England, would very likely have been observed and reported. A more detailed view of the predictions of both the Forecast and Reference Models, for inundation near Mill Cove by a magnitude 9.0 event north of Puerto Rico, is provided in Figure 16. The agreement between models is good, though there is a suggestion that the coarser representation of the Casco Bay Bridge in the forecast model may be over-attenuating the westward passage of wave energy. The channels beneath the

bridge stand out in Figure 15 as having the potential for severe current oscillations and speeds. Depth adjustments to the relatively coarse grid were aimed at correcting instabilities rather than accurately replicating flows. Given its proximity to Mill Cove, follow-up studies on whether the forecast model representation of the bridge pilings creates an excessive barrier should be performed now that the initial version is complete.

While Mill Cove is the location most at risk of inundation, particularly for lower magnitude sources, other areas are threatened. Shaded in red in Figure 17 are areas inundated (above the MHW water line) within the C-grid domain by a magnitude 9.0 event, centered on unit source B51 (see Figure 14.) The inset panel in the lower left illustrates the dependence of total inundated area (in square kilometers) on source magnitude, as derived from Forecast Model simulations. At magnitude 8.7 and above an area in East Deering, near the southern approaches of Highway 1 to the Martin Point Bridge at the mouth of the Presumpscot Estuary, becomes subject to inundation. Mill Cove, at an antinode of one of the harbor oscillation modes, experiences inundation, at lower source magnitudes, than elsewhere. The non-linear dependence of inundation there on source magnitude is further illustrated in Figure 18. Again it should be emphasized that these simulations, and those that follow, are intended to be illustrative, rather than a definitive risk assessment.

Mackworth Island, north of the entrance to the Presumpscot River Estuary is a recreational rather than a residential site. It is joined to the mainland by a causeway that, in the digital elevation model employed, stands less that one meter above MHW. Together with the shoreline leading to Waites Landing, an embayment is formed that appears capable of water level fluctuations of overtopping the causeway. The situation, though perhaps a low probability coincidence of a major tsunami and high tide, is illustrated in Figure 19. Of note though is the good agreement between the forecast and reference model solutions.

Extreme current speeds are likely to be of concern to an area with so many marinas and major water-related activity: ferries cruise ships and oil tanker traffic. Portland is the largest oil port on the eastern seaboard and the terminus of the Portland-Montreal Pipe Line that brings more than 200 oil tankers to the South Portland facility in a year. The tank farm appears to be well protected by berms (see Figure 20) but the effect of severe currents or grounding must be of concern to terminal operators. The twin basins straddling the jetty itself are quite deep. However the forecast model as designed assumes a water level standing at MHW in order to provide worst-case inundation estimates. A variant that treated the opposite extreme of low water conditions could be investigated since the large tidal range of Portland might induce instabilities not present in the high water setup. There are some differences between the forecast and reference model predictions, shown in Figure 20, for the extent of severe current speed conditions on either side of the docking area. The sharp depth gradients present in the DEM near the jetty and at other points in the C-grid domain (near State Pier, a channel leading to the Coast Guard Base, and other dredged areas) required smoothing in the forecast model in order to avoid instability.

In conclusion, Forecast and Reference Models for tsunami impact on Portland, Maine have been developed and tested. Unlike similar modeling for threatened coastal communities in the Pacific basin, where tide gage observations of historic events are available for model validation, no such data exist for Portland. The Portland models, apart from site-specific bathymetry, employ the same numerical codes and parameters as employed where success under operational conditions has been demonstrated. Simulations indicate that Portland's protected location within Casco Bay, itself a shielded sub-region of the Gulf of Maine, limits its vulnerability mainly to more severe, seismically generated, tsunami events that might occur north of Puerto Rico. Nonetheless, the strong directionality that tsunami energy propagation may exhibit, and the potential impact that tsunami-generated currents might have on the marine-intense infrastructure of the area makes the addition of forecast capability by the Tsunami Warning Centers an important element of a comprehensive emergency management plan for Portland. Additionally, used as part of a public awareness and education program, or in risk assessment, the Forecast model should assist in making the Portland metropolitan area "TsunamiReady" (www.tsunamiready.noaa.gov).

7 Acknowledgments

The image used for Figure 1 was accessed from Wikipedia (User: "Tye dye 9205"). The author wishes to acknowledge use of the Ferret program (a product of NOAA's Pacific Marine Environmental Laboratory, freely available at ferret.pmel.noaa.gov/Ferret/.) for analysis and graphics. Google Earth and Google Maps were heavily used to visualize the study area. This publication is partially funded by the Joint Institute for the study of the Atmosphere and Ocean (JISAO) under NOAA Cooperative Agreement No. NA17RJ1232, JISAO Contribution No. XXXX. This is PMEL Contribution No. NNNN

8 References

Atlantic and Gulf of Mexico Tsunami Hazard Assessment Group (AMTHAG), (2008): Evaluation of Tsunami Sources with the Potential to Impact the U.S. Atlantic and Gulf Coasts — An Updated Report to the Nuclear Regulatory Commission. U.S.G.S. Administrative. Report: 300 pp.

Barkan, R., U.S. ten Brink, and J. Lin (2009): Far field tsunami simulations of the 1755 Lisbon earthquake: Implications for tsunami hazard to the U.S. East Coast and the Caribbean. *Marine Geology 264*, 109-122.

Boston Globe (2008): Massive waves a mystery at Maine harbor. www.boston.com/news/local/maine/articles/2008/11/04/massive_waves_a_mystery_at_maine_harbor/

Bond, N.A., J.E. Overland, M. Spillane, and P.J. Stabeno (2003): Recent shifts in the state of the North Pacific. *Geophys. Res. Lett.*, *30*(23), 2183, doi: 10.1029/2003GL018597.

Budd, B. (1980): A Local Archive of Top Tides and Tidal Surges for Portland, Maine. [Available at NWS, 1 Weather La., Gray, ME 04039.]

Cannon, J.W. (2007): Northern New England Coastal Flooding. GoMOOS Newsletter, Spring 2007. www.gomoos.org/aboutgomoos/coastalfloodwafpreprint.pdf

Conforti, J.A. (2005): Creating Portland: History and Place in Northern New England. Hanover NH, University Press of New England, 348p.

Cotterly, W. (1996): Hurricanes & Tropical Storms: Their Impact on Maine and Androscoggin County. http://www.pivot.net/~cotterly/hurricane.PDF

DiPhilippo, K. 2007: The Grist Mill and Ship Yard Point. South Portland Historical Society article published June 29, 2007 in the *South Portland Sentry* and archived at www.sphistory.org/ .

Driscoll, N.W., Weissel, J.K., and Goff, J.A., 2000, Potential for large-scale submarine slope failure and tsunami generation along the US mid-Atlantic Coast. *Geology 28*, (5), 407-410.

Fine, I.V., A.B. Rabinovich, B.D. Bornhold, R.E. Thomson, and E.A. Kulikov (2005): The Grand Banks landslide-generated tsunami of November 18, 1929: preliminary analysis and numerical modeling. *Marine Geology 215*, 45–57.

Gica, E., M. Spillane, V.V. Titov, C.D. Chamberlin, and J.C. Newman (2008): Development of the forecast propagation database for NOAA's Short-term

Inundation Forecast for Tsunamis (SIFT). NOAA Tech. Memo. OAR PMEL-139, NTIS: PB2008-109391, 89 pp.

Lander, J.F., and P.A. Lockridge (1989): United States Tsunamis, 1690 to 1988, Publ. 41–2. National Geophysical Data Center, Boulder, CO, 265 pp.

Lim, E., L.A. Taylor, B.W. Eakins, K.S. Carignan, R.R. Warnken, and P.R. Medley (2008): Digital elevation model of Portland, Maine: Procedures, data sources and analysis. www.ngdc.noaa.gov/mgg/inundation/tsunami/data/portland_me/portland_me.pdf

Monserrat, S., I. Vilibic´, and A. B. Rabinovich (2006): Meteotsunamis: atmospherically induced destructive ocean waves in the tsunami frequency band. *Nat. Hazards Earth Syst. Sci., 6*, 1035–1051.

Percival, D.B., D. Arcas, D.W. Denbo, M.C. Eble, E. Gica, H.O. Mofjeld, M.C. Spillane, L. Tang, and V.V. Titov (2009): Extracting tsunami source parameters via inversion of DART® buoy data. NOAA Tech. Memo. OAR PMEL-144, 22 pp.

Sallenger, A.H, Jr., J.H.List, G. Gelfenbaum, R.P. Stumpf, and M. Hansen (1995): Large Wave at Daytona Beach, Florida, Explained as a Squall-line Surge. *J. Coastal Res., 11*(4), 1383-1388.

Spillane, M.C., E. Gica, V.V. Titov, and H.O. Mofjeld (2008): Tsunameter network design for the U.S. DART® arrays in the Pacific and Atlantic Oceans. NOAA Tech. Memo. OAR PMEL-143, 165 pp.

Sweet, W., C. Zervas, and S. Gill (2009): Elevated East Coast Sea level anomaly, June-July 2009. NOAA Tech. Report NOS CO-OPS 051, August 2009. tidesandcurrents.noaa.gov/publications/EastCoastSeaLevelAnomaly_2009.pdf

ten Brink, U.S., Lee, H.J., Geist, E.L., Twichell, D.C., (2009): Assessment of tsunami hazard to the U.S. East Coast using relationships between submarine landslides and earthquakes. *Mar. Geol. 264*, 65–73

Titov, V., and F.I. González (1997): Implementation and testing of the Method of Splitting Tsunami (MOST) model. NOAA Tech. Memo. ERL PMEL-112, NTIS: PB98-122773, NOAA/Pacific Marine Environmental Laboratory, Seattle, WA, 11 pp.

Titov, V.V., and C.E. Synolakis (1998): Numerical modeling of tidal wave runup. *J. Waterw. Port Coast. Ocean Eng.*, *124*(4), 157–171.

Wei, Y., E. Bernard, L. Tang, R. Weiss, V. Titov, C. Moore, M. Spillane, M. Hopkins, and U. Kânoğlu (2008): Real-time experimental forecast of the Peruvian tsunami of August 2007 for U.S. coastlines. *Geophys. Res. Lett.*, *35*, L04609, doi: 10.1029/2007GL032250.

Wessel, P. (2008) Analysis of observed and predicted tsunami travel times for the Pacific and Indian Oceans. *Pure Appl. Geophys 166*, 301-324, DOI 10.1007/s00024-008-0437-2.

Wigen, S.O. (1989) Report on the Assessment and Documentation of Tsunamis for Eastern Canada. Unpublished Manuscript. Tide and Tsunami Services, Fulford Harbour, B.C., 16 pp.

Grid Area	**Portland, Maine**
Coverage Area	70.74^0 to 69.63^0W, 43.00^0 to 43.99^0N
Coordinate System	Geographic decimal degrees
Horizontal Datum	World Geodetic System 1984 (WGS84)
Vertical Datum	**Mean High Water (MHW)**
Vertical Units	Meters
Cell Size	**1/3 arc-second**
Grid Format	ESRI Arc ASCII grid

Portland, Casco Bay, ME	**Station#8418150**	**$43^0$39.4'N, $70^0$14.8W** 43.656039,-70.245991	
Tidal Datum and Range Values (Epoch 1983-2001)			
MHHW (Mean Higher High)	5.626m	Diurnal Range 3.019m	
MHW (Mean High Water)	5.493m		Mean Range 2.781m
MSL (Mean Sea Level)	4.113m		
MLW (Mean Low Water)	2.712m		
MLLW (Mean Lower Low)	2.607m		
Sea Level Trends and Cycles			
Long Term SL Trend	Increasing 1.82±0.17mm/year		
Seasonal Cycle Range	Minimum -38mm(January); Maximum 30mm(June)		
Interannual Variation	Minimum -9mm(1990); Maximum +11mm(1971)		
Benchmark for Coastal Flooding by Storm Surge (www.gomoos.org)			
Sea levels of 3.658m (12ft) or more above MLLW			

Grid	Zonal Extent (W)		Meridional Extent (N)		Resolution (“)		Values EW x NS	
					RM	FM	RM	FM
A	72^0	63^0	37^0	$46^015'$	30	120x90	1081x1111	271x371
B	$70^036'$	$69^030'$	$43^015'$	$43^054'$	3	12x9	1321x781	331x261
C	$70^018'50"$	$70^011'18"$	$43^033'58"$	$43^043'30"$	0.33	1.33x1	1357x1717	280x537
	$70^017'30"$			$43^042'54"$				

Grid	Filename	Maximum Depth (m)	Minimum CFL (s)	Model Time Step (s)	Water Cells
A	GulfME_30s_r	5670	3.064	1.875 (4x)	899892
	GulfME_120s90s_f	5662	11.814	7.5 (4x)	74945
B	CascoBay_3s_r	219.3	1.409	0.9375 (2x)	695489
	CascoBay_12s9s_f	210.6	5.942	3.75 (2x)	56917
C	PortlandME_1th_r	25.01	0.4767	0.46875	717185
	PortlandME_4th_f	24.99	1.908	1.875	54642

Scenario Name	Source Zone	Tsunami Source	α [m]
	Micro-tsunami ("Null") Scenarios		
Caribbean	**Atlantic**	**A47-A55, B47-B55**	**10^{-4}**
South Sandwich	South Atlantic	A1-A5, B1-B5	10^{-4}
Cadiz "Wedge"	Lisbon 1755 Candidate	139x200km,Strike 345º	$3.6x10^{-4}$
	Mega-tsunami (M_w 9.0) Scenarios		
Caribbean	**Atlantic**	**A47-A55, B47-B55**	**9.86**
South Sandwich	**South Atlantic**	**A1-A5, B1-B5**	**9.86**
Cadiz "Wedge"	**Lisbon 1755 Candidate**	**139x200km,Strike 345º**	**31.92**
	Major Tsunami (M_w 8.83) Scenarios		
Caribbean/Atlantic	Atlantic	39 groups of 5 A,B pairs	10
South Sandwich	South Atlantic	A1-A5, B1-B5	10
Cadiz "Wedge"	Lisbon 1755 Candidate	139x200km,Strike 345º	18.0
Gorringe Bank	Lisbon 1755 Candidate	125x60km, Strike 51º	66.7
Horseshoe Fault	Lisbon 1755 Candidate	106x70km. Strike 41º	67.4
Lisbon	Lisbon 1755 Candidate	210x75km, Strike 334º	31.7
Portimao	Lisbon 1755 Candidate	102x50, Strike 274º	98.0
	M_w 7.5 Scenarios		
Atlantic	Atlantic/Caribbean	B1, …, B92 individually	1
	M_w 8.0 Scenarios		
Atlantic	Atlantic/Caribbean	B2, …, B91 groups of 3	1.87
	M_w 8.5 Scenarios		
Atlantic	Atlantic/Caribbean	B3, …, B90 groups of 5	6.33


Waites Landing
Presumpscot River Estuary
East Deering
Mackworth Island
Back Cove
Eastern Promenade
Little Diamond Island
Fort Gorges
Portland
State Pier
Spring Pt. Ledge Light
I-295 Bridge
Fore River
Fort Preble
House Island
Portland Int.Jetport
Casco Bay Bridge
Hwy-1 Bridge
Mill Cove
Long Creek
South Portland
Cushing Island
Cape Cottage
Portland Head Light

Bar Harbor ME

Portsmouth NH

Gulf of Maine

Cape Bonavista

Newfoundland 1929

Portland

Meteorological Forcing

Portland

Cape Small

Casco Bay

Cape Elizabeth

Submarine Landslide

East Atlantic

Lisbon 1755

La Palma Subaerial Landslide

South Atlantic

South Sandwich Island Arc

Puerto Rico Trench

Caribbean

Adapted from Google Maps

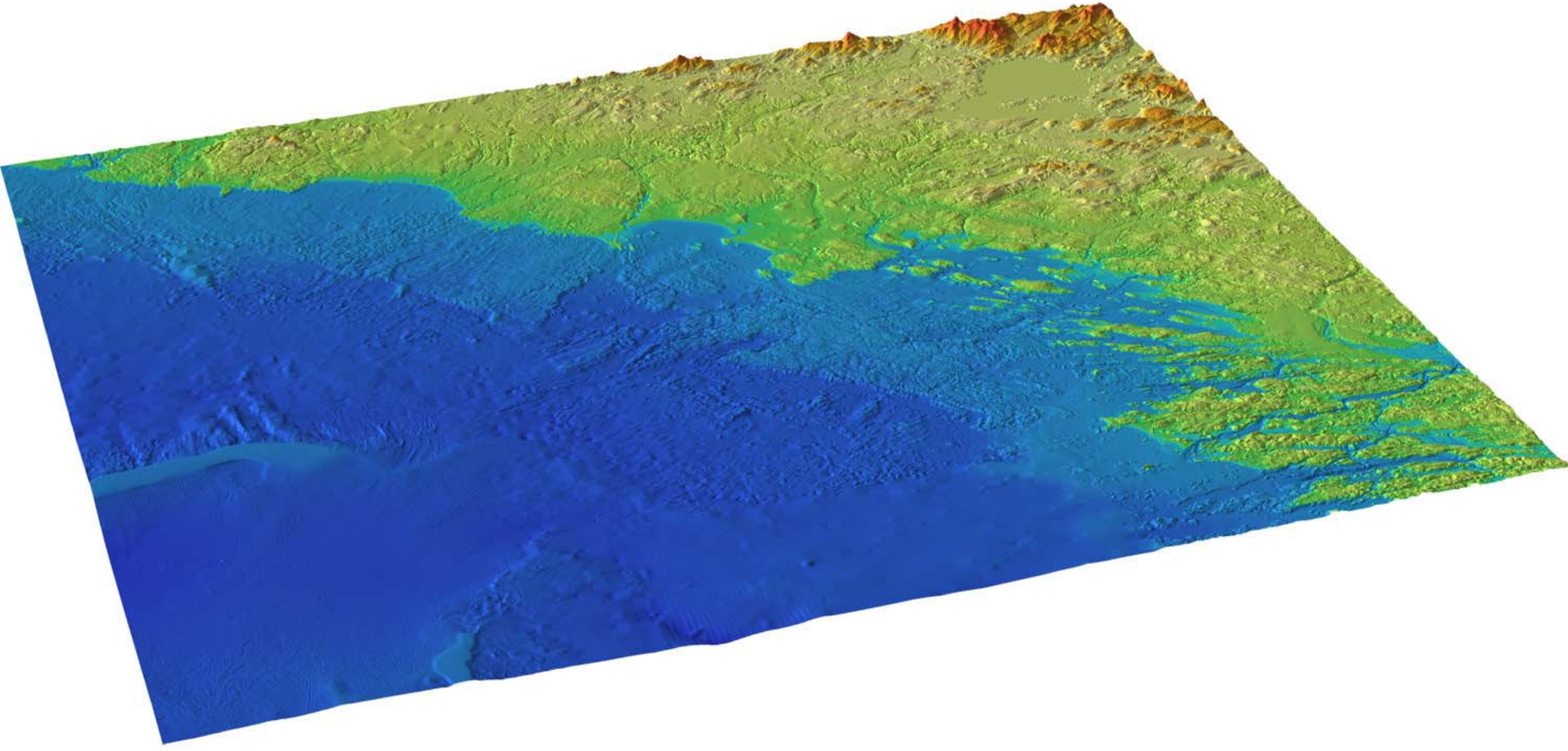

Display:
1 min | **6 min** | **6 min alt** | **Predicted**

From: Sep 22 2009 0714 *hhmm*

Retrieve: Data Listing | Import to Excel

To: Sep 23 2009 0714 *hhmm*

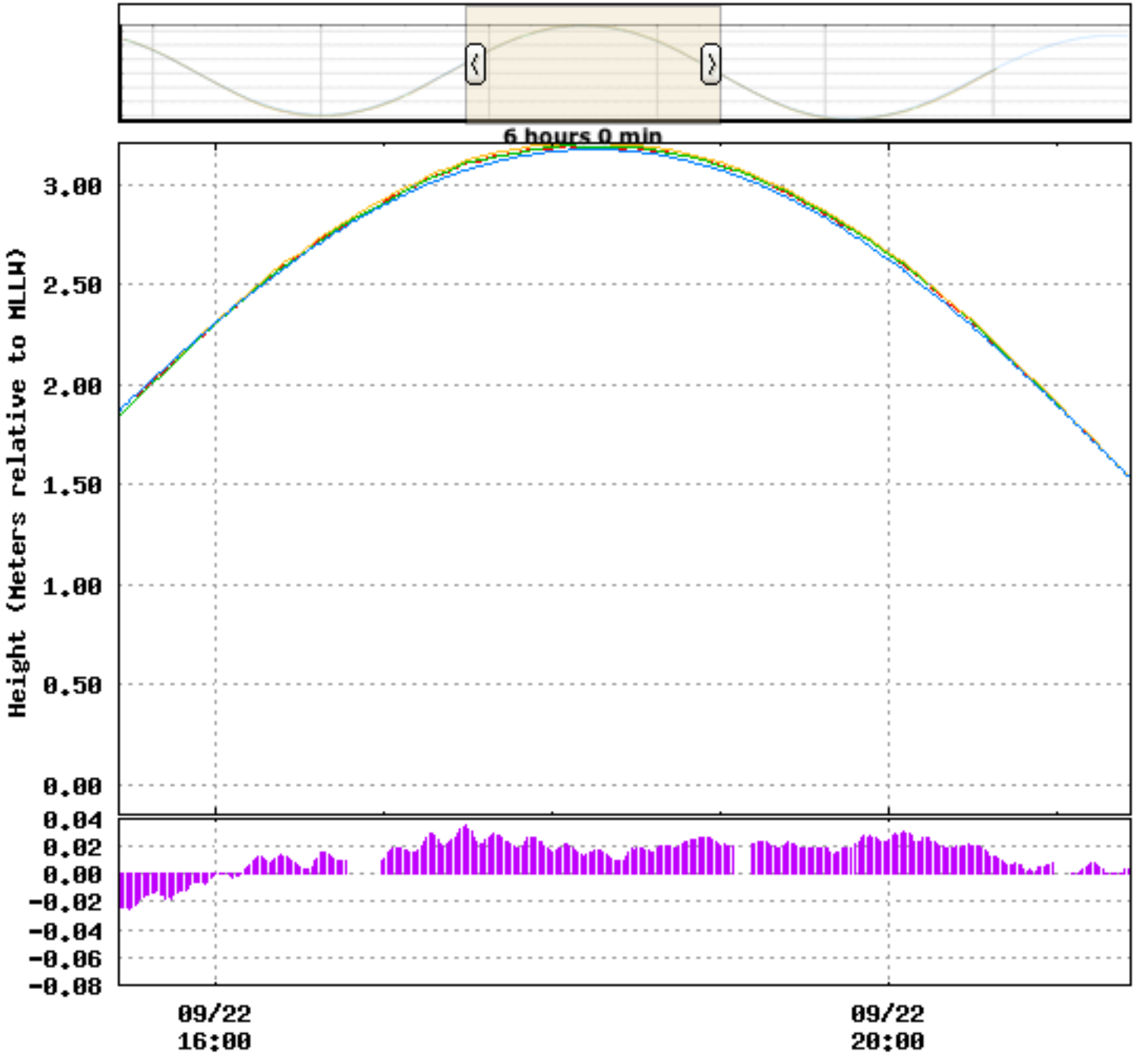

Hint: Click and drag the tan slider or the plot

Water levels for 8418150 - Portland
From 09/22/2009 07:14 through 09/23/2009 07:14
Disseminating sensor: A1 | Alternate sensor: B1 | Datum: MLLW

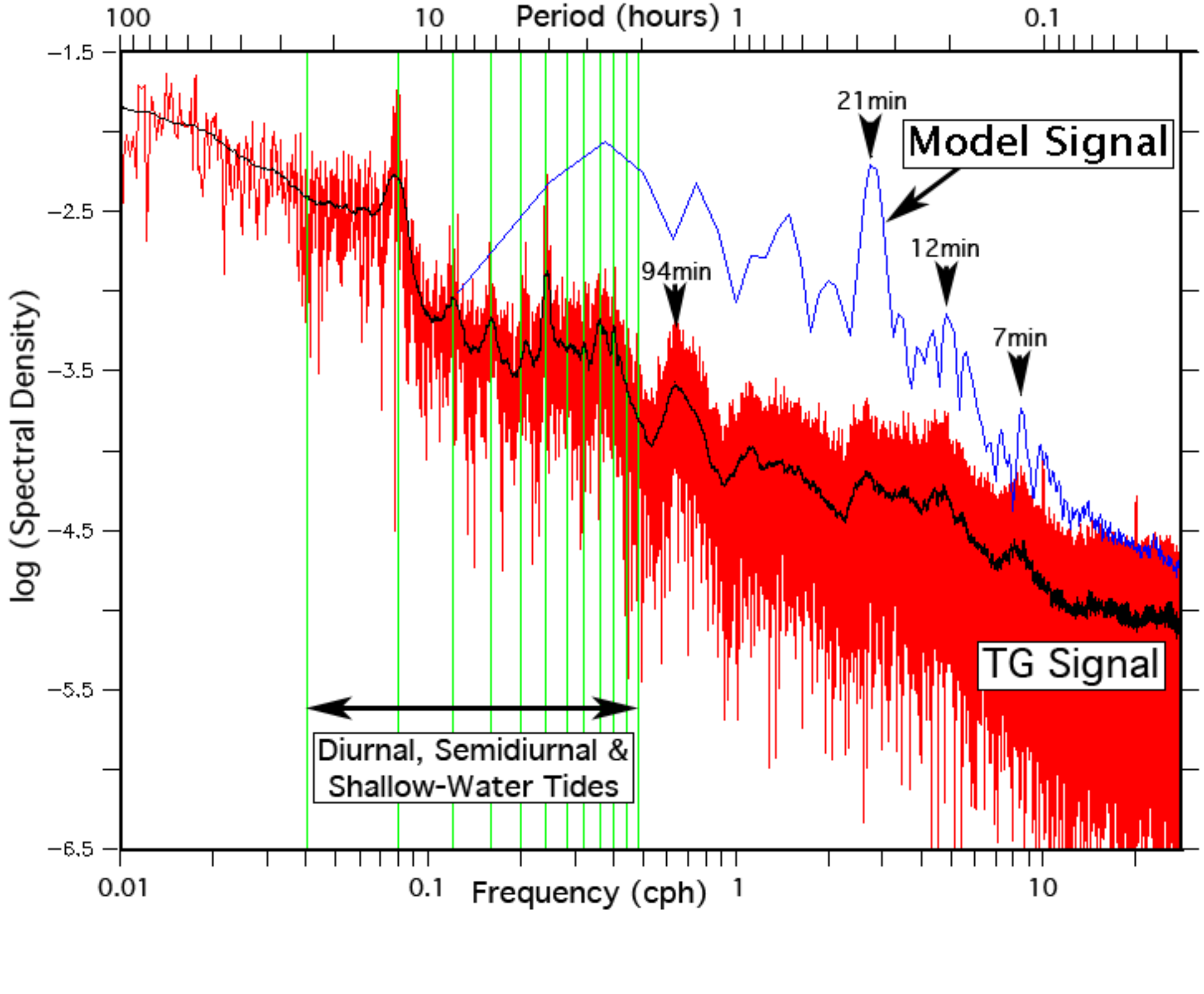
100
10
Period (hours)
1
0.1
−1.5
−2.5
−3.5
−4.5
−5.5
−6.5
log (Spectral Density)
21min
Model Signal
12min
94min
7min
TG Signal
Diurnal, Semidiurnal &
Shallow-Water Tides
0.01
0.1
Frequency (cph)
1
10

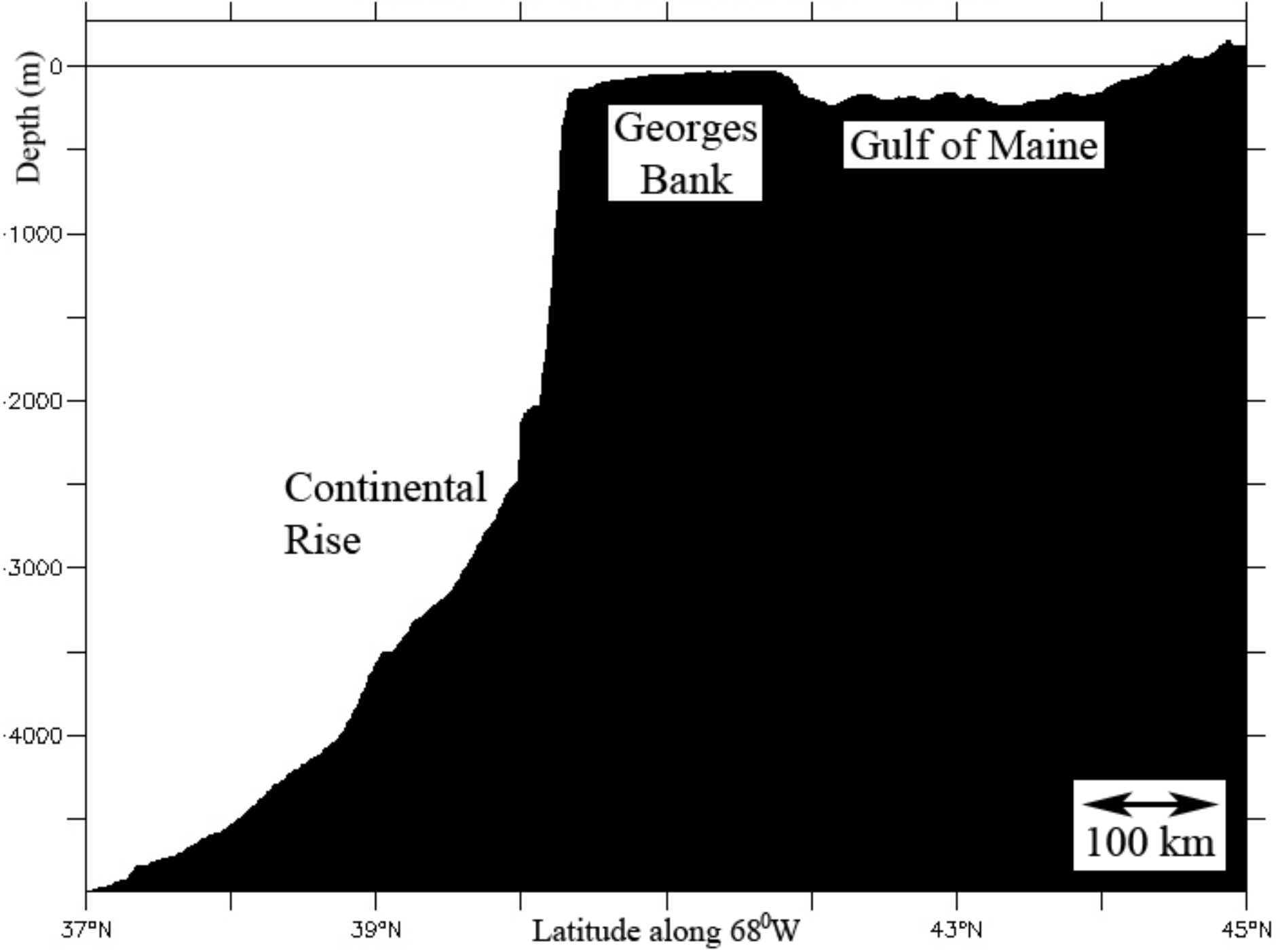
Depth (m)
0
-1000
-2000
-3000
-4000
Georges Bank
Gulf of Maine
Continental Rise
100 km
37°N
39°N
Latitude along 68°W
43°N
45°N

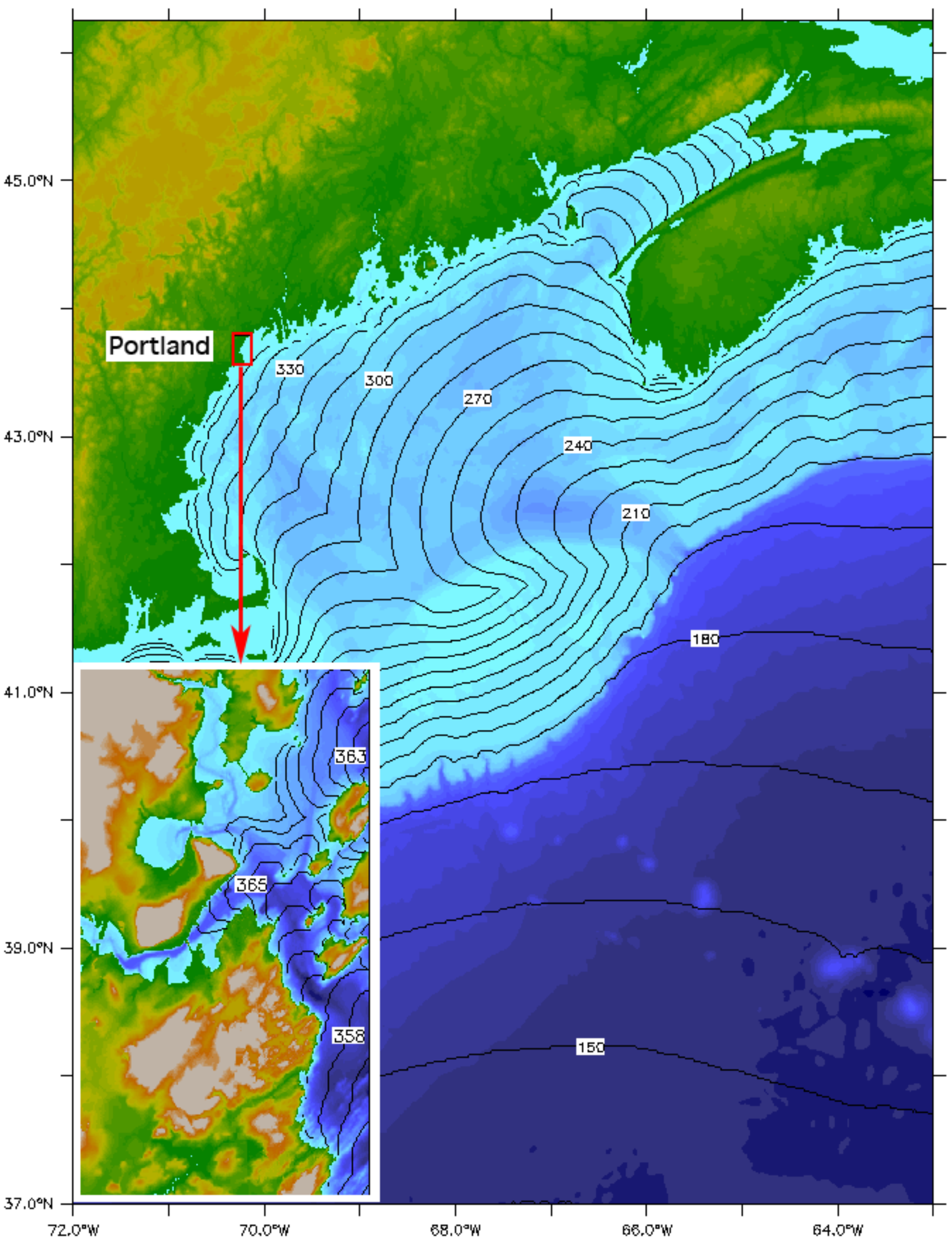
Portland
330
300
270
240
210
180
150
363
365
358
45.0°N
43.0°N
41.0°N
39.0°N
37.0°N
72.0°W
70.0°W
68.0°W
66.0°W
64.0°W

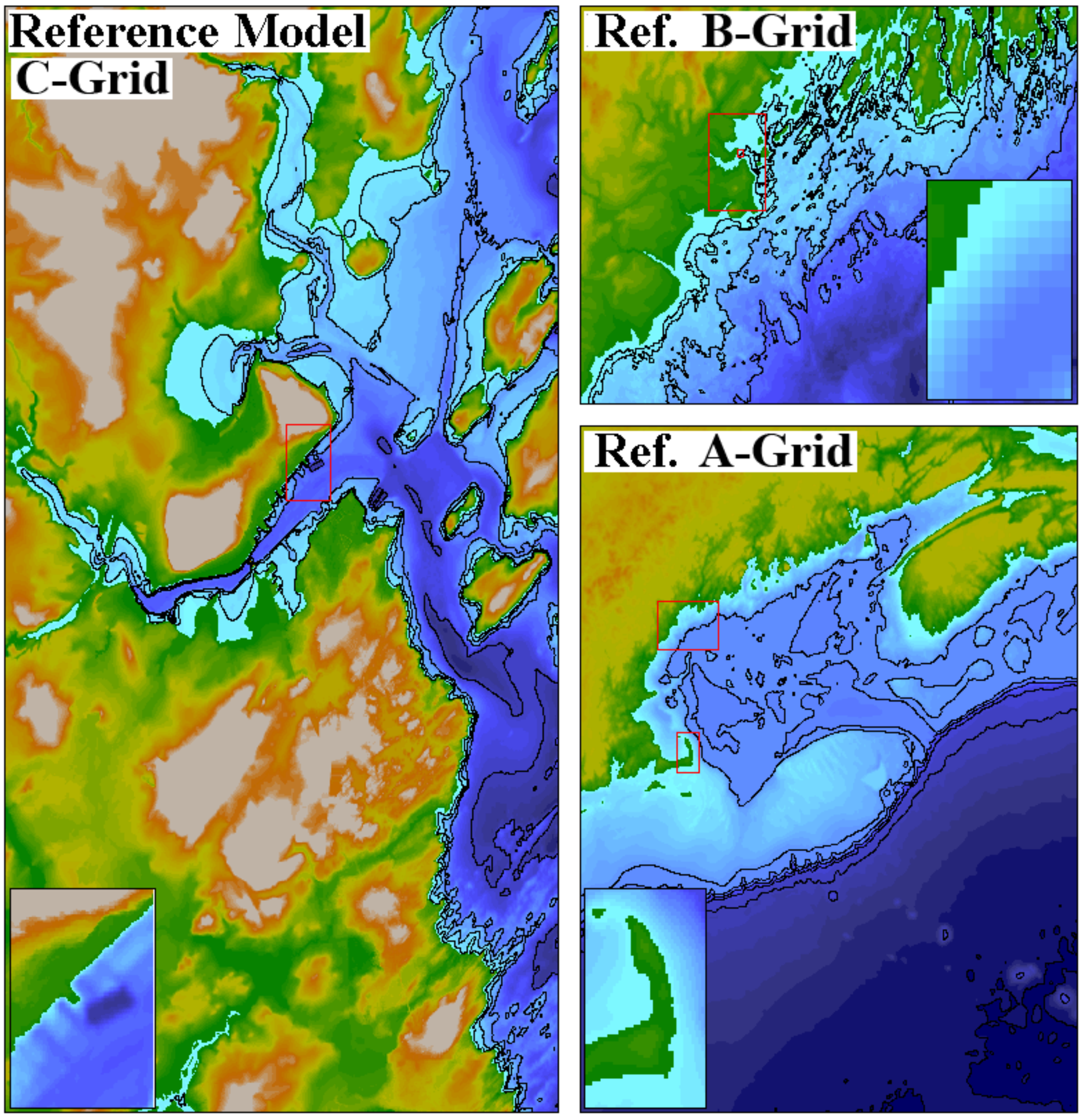
Reference Model
C-Grid
Ref. B-Grid
Ref. A-Grid

Forecast Model

C-Grid

Fcst. B-Grid

Fcst. A-Grid

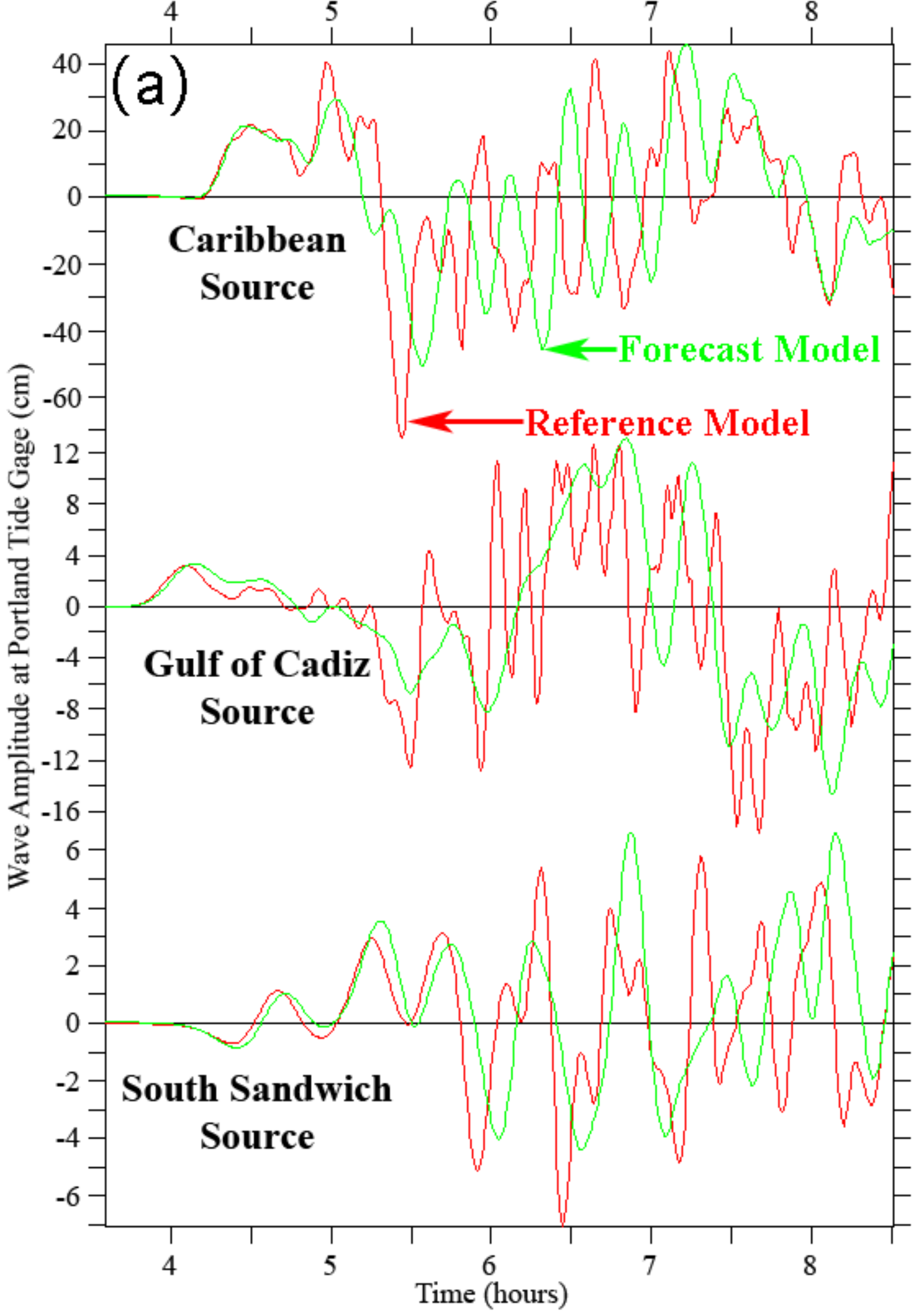
(a)
Caribbean Source
Forecast Model
Reference Model
Gulf of Cadiz Source
South Sandwich Source
Wave Amplitude at Portland Tide Gage (cm)
Time (hours)
40
20
0
-20
-40
-60
12
8
4
0
-4
-8
-12
-16
6
4
2
0
-2
-4
-6
4
5
6
7
8

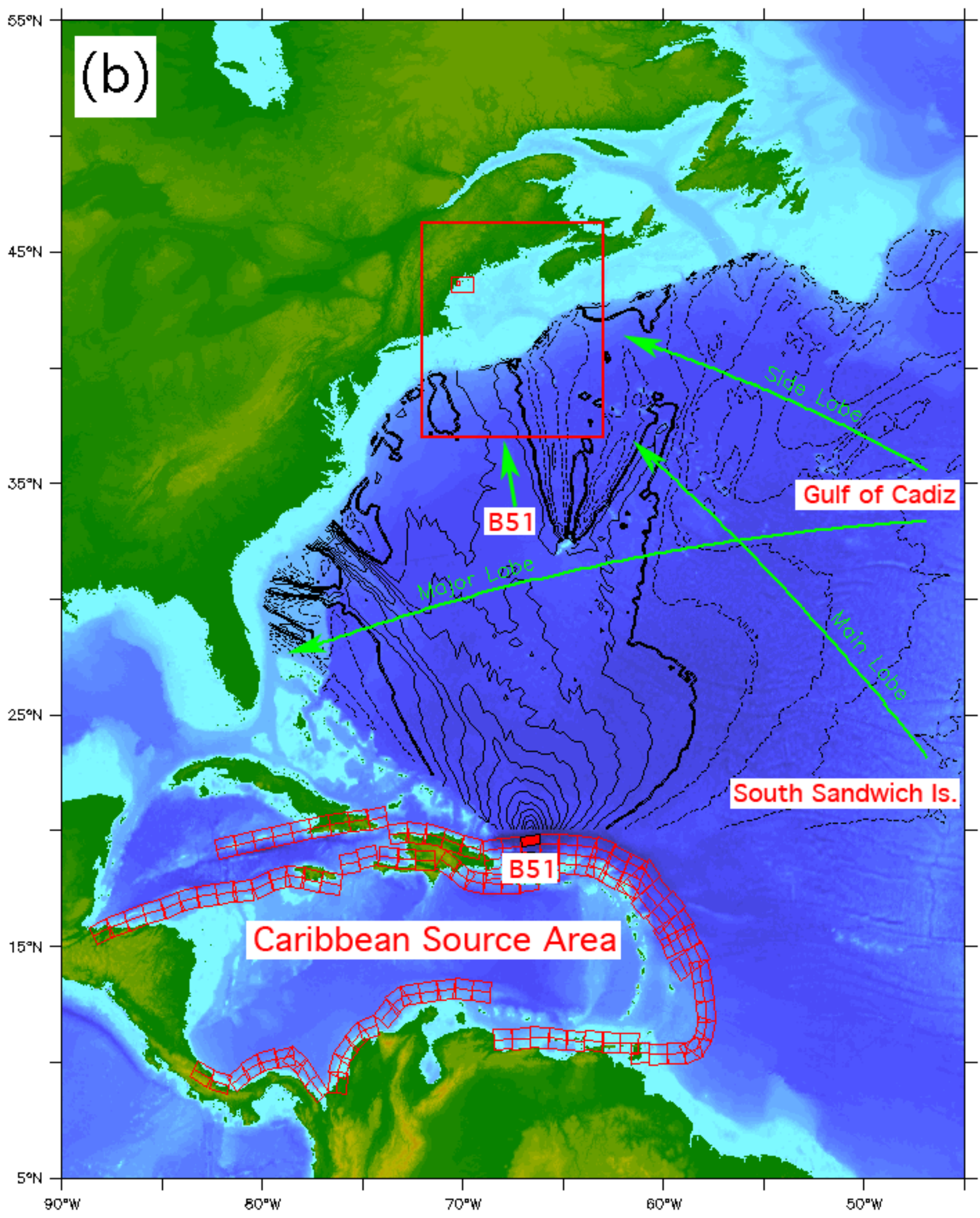
(b)
55°N
45°N
35°N
25°N
15°N
5°N
90°W
80°W
70°W
60°W
50°W
B51
Side Lobe
Gulf of Cadiz
Major Lobe
Main Lobe
South Sandwich Is.
B51
Caribbean Source Area

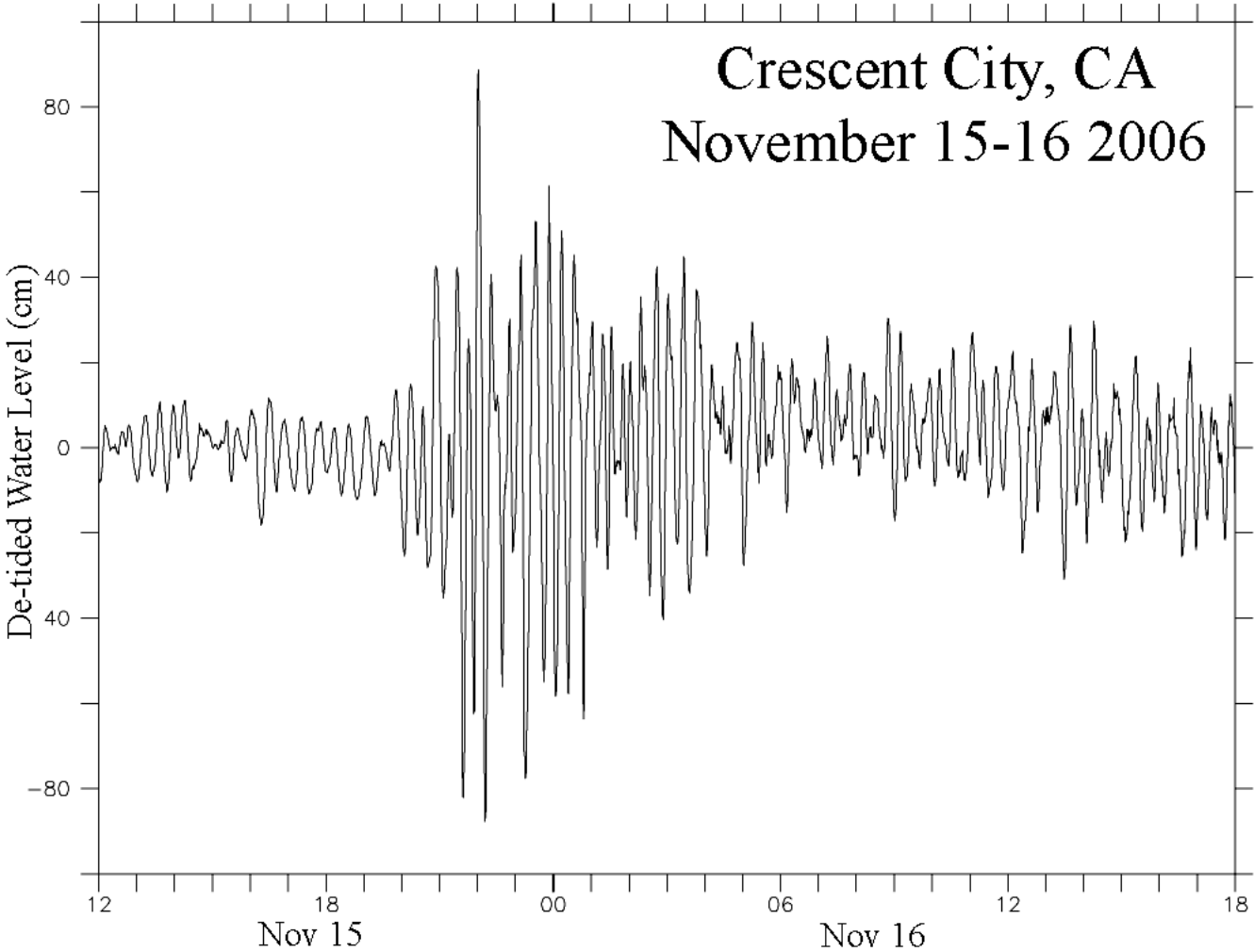
Crescent City, CA
November 15-16 2006
De-tided Water Level (cm)
80
40
0
40
−80
12
18
00
06
12
18
Nov 15
Nov 16

(a)

12
10
8
6
4

Mode-1 (56.3%)

(b)

Mode-2

Mode-1

Mode-3

2
4
6
8
10
12
14
16
18
20

-6
-4
-2
0
2
4
6

Amplitude

Time

(c)

(d)

15
10
5
0
-5
-10

Mode-2 (20.4%)

10
8
6
4
2
0
-2
-4
-6

Mode-3 (9.9%)

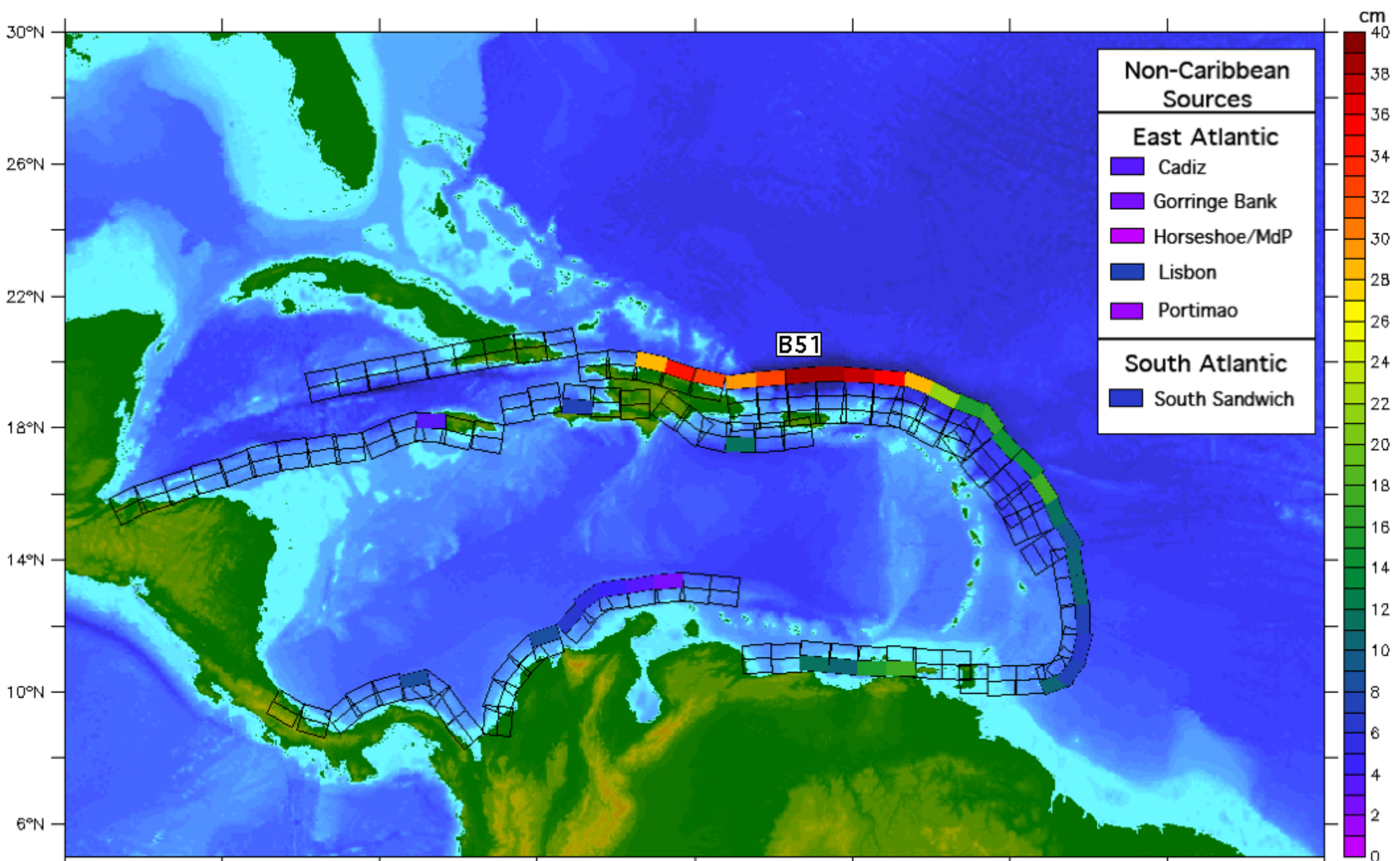
Non-Caribbean Sources
East Atlantic
Cadiz
Gorringe Bank
Horseshoe/MdP
Lisbon
Portimao
South Atlantic
South Sandwich
B51
cm
40
38
36
34
32
30
28
26
24
22
20
18
16
14
12
10
8
6
4
2
0
30°N
26°N
22°N
18°N
14°N
10°N
6°N
90°W
80°W
70°W
60°W
50°W

Amplitude

Speed

Forecast Model Results

Maximum Amplitude (cm) 10 20 30 40 50 60 70 80 90 100 Maximum Speeds (cm/s)

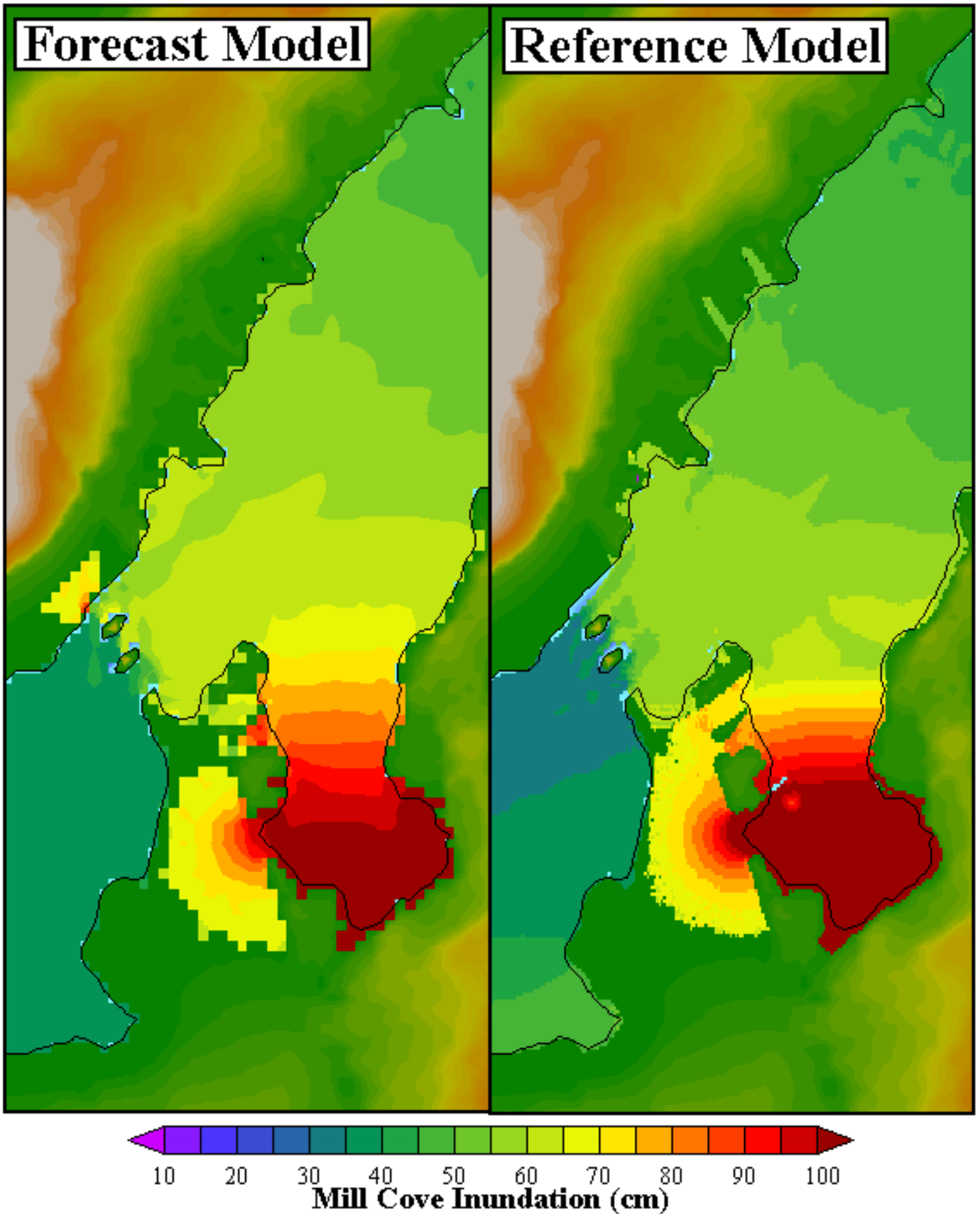
Forecast Model
Reference Model
10
20
30
40
50
60
70
80
90
100
Mill Cove Inundation (cm)

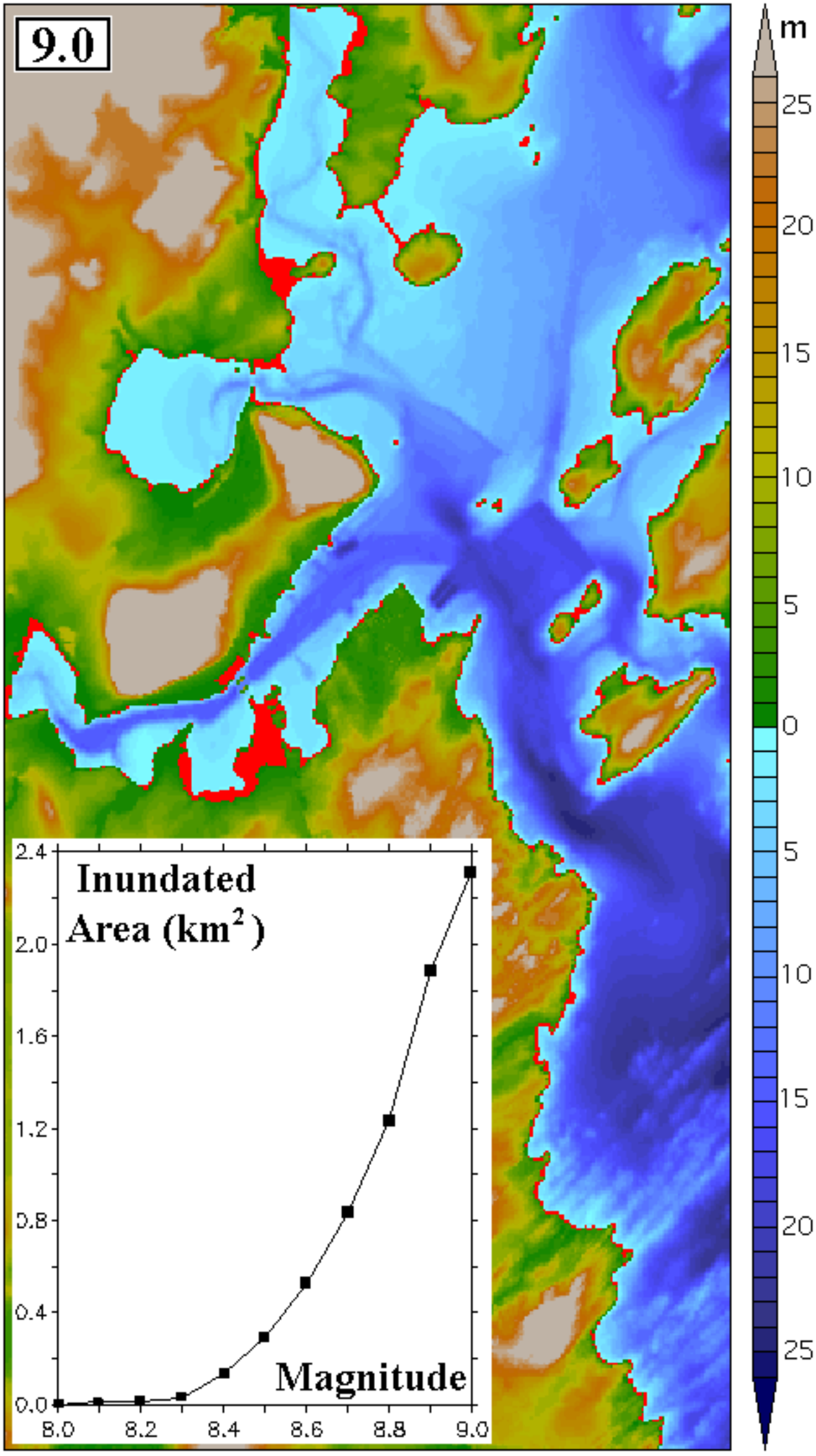
9.0
m
25
20
15
10
5
0
5
10
15
20
25
Inundated
Area (km²)
2.4
2.0
1.6
1.2
0.8
0.4
0.0
8.0
8.2
8.4
8.6
8.8
9.0
Magnitude

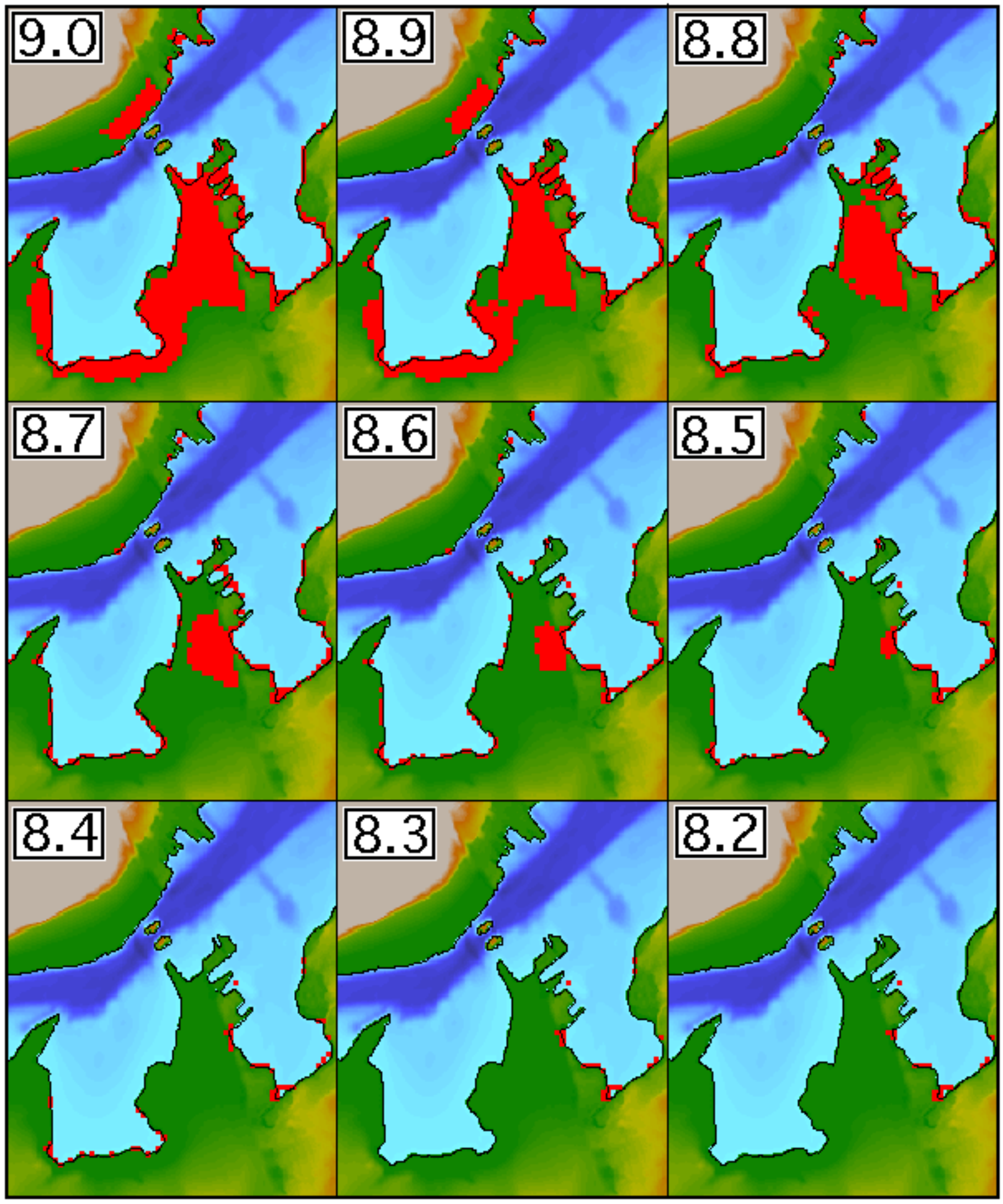
9.0
8.9
8.8
8.7
8.6
8.5
8.4
8.3
8.2

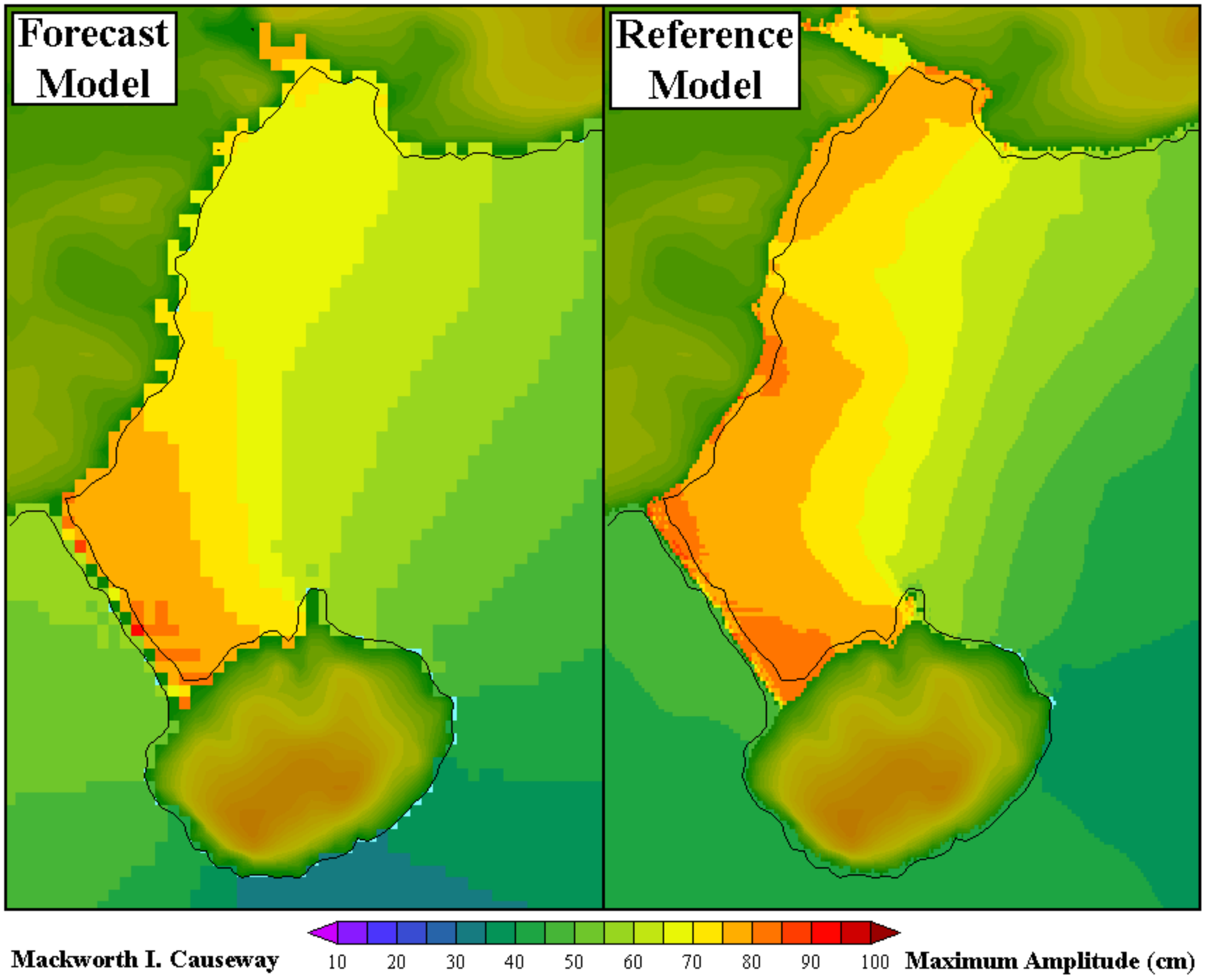
Forecast Model
Reference Model
Mackworth I. Causeway
10
20
30
40
50
60
70
80
90
100
Maximum Amplitude (cm)

Forecast Model

Reference Model

100
90
80
70
60
50
40
30
20
10

Maximum Speeds (cm/s) for $M_w = 9.0$ Caribbean Event

Appendix A: Model input file for Portland, Maine.

The following table contains the parameter and file choices used in the input file for the SIFT implementation (most3_facts_nc.in) of the optimized forecast model for Portland, Maine.

Parameter/File*	**Purpose**
0.0001	Minimum amp. of input offshore wave (m)
1.0	Minimum depth of offshore (m)
0.1	Dry land depth of inundation (m)
0.0009	Friction coefficient (n**2)
1	Let A-Grid and B-Grid run up
90.0	Max eta before blow-up (m)
1.875	Time step (sec)
23040	Total number of time steps in run
4	Time steps between A-Grid computations
2	Time steps between B-Grid computations
16	Time steps between output steps
16	Time steps before saving first output step
1	Save output every n-th grid point
portland_run2d/GulfME_120s90s_f.most	A-grid bathymetry file
portland_run2d/CascoBay_12s9s_f.most	B-grid bathymetry file
portland_run2d/PortlandME_4th_f.most	C-grid bathymetry file
./	Directory of source files
,/	Directory for output files

* The column headings are not part of most3_facts_nc.in